SOVIET PHYSICS USPEKHI VOLUME 12, NUMBER 4 JANUARY-FEBRUARY 1970

535.375

STIMULATED MANDEL'SHTAM-BRILLOUIN SCATTERING AND STIMULATED ENTROPY (TEMPERATURE) SCATTERING OF LIGHT

V. S. STARUNOV and I. L. FABELINSKIĬ

P. N. Lebedev Physics Institute, USSR Academy of Sciences

Usp. Fiz. Nauk 98, 441–491 (July, 1969)

I. INTRODUCTION

THE study of the spectra of scattered light was initiated more than forty years ago, and the main features of various spectra of thermal radiation were determined before the appearance of various laser excitation sources.[1] Studies were made of the spectra of Raman scattering of light and of the spectra of scattering due to the time variation of the fluctuations of the dielectric constant as the result of thermal fluctuations of pressure (Mandel'shtam-Brillouin scattering), fluctuations of entropy (the central component of the fine structure of the Rayleigh line), and anisotropy fluctuations (the wing of the Rayleigh line).

The use of gas lasers and powerful light pulses from solid-state lasers has made it possible to increase the volume of information obtained by studying the spectra of scattered light, and to observe many new phenomena[1-3]. When scattering is excited by a giant laser pulse, the aforementioned four types of scattering give rise to new phenomena—stimulated Raman scattering of light[4] (1963), stimulated Mandel'shtam-Brillouin scattering[5] (1964), stimulated scattering of light in the Rayleigh-line wing[6] (1965), and stimulated entropy (temperature) scattering[7] (1967). Effects of self-focusing[8], which are genetically connected with certain types of stimulated scattering, were observed. Spectral shifts and broadening of the spectrum of a light pulse, resulting from phase modulation due to temporal variation of the nonlinear part of the refractive index were found[9]. All these and many other optical phenomena occurring when intense light propagates through matter make up a new branch of physics, called nonlinear optics[1-3,10].

The present article is devoted to an exposition of the main results of theoretical and experimental investigations of stimulated Mandel'shtam-Brillouin scattering (SMBS) and stimulated entropy (temperature) scattering of light (STS).

The spectrum of thermal* scattering of light contains, as a result of adiabatic density fluctuations (pressure fluctuations) on both sides of the unshifted lines, Mandel'shtam-Brillouin components[1,11,12], whose shift Ω_{MB} and the width $2\delta\Omega_{MB}$ are determined by the relations

$$\Omega_{MB} = \pm 2n\frac{v}{c}\omega_0 \sin\frac{\vartheta}{2}, \qquad 2\delta\Omega_{MB} = 2\alpha v; \tag{1}$$

here n, ϑ, v, and α are the refractive index of the medium, the scattering angle, the velocity of hypersound, and the amplitude coefficient of absorption of sound of frequency Ω_{MB}, while ω_0 and c are the frequency and velocity of light in vacuum.

Scattering of light as the result of isobaric fluctuations of density (entropy fluctuations) is represented in the spectrum by an undisplaced line of the Rayleigh triplet with half-width

$$2\delta\Omega_c = 2\chi|\mathbf{k}_0 - \mathbf{k}_s|^2 = 2\chi q^2, \tag{2}$$

where χ is the temperature-conductivity coefficient and $\mathbf{k}_0$ and $\mathbf{k}_S$ are the wave vectors of the exciting and scattered light.

In experimental and theoretical studies of the thermal-scattering spectra, account is taken of the influence of the thermal motion in the medium on the light wave, but the action of the light wave on the motion in the medium is neglected. The situation changes if the scattering is excited by a powerful light pulse from a laser. In this case the intensity of the electric field of the exciting light wave is so high ($\sim 10^4$–10^8 V/cm), that this field, together with the field of the initial weak thermal scattering, begins to exert a strong influence on the character of the motion in the medium. As a result of the electrostriction effect, these fields will lead, under certain conditions, to an increase of the intensity of the sound wave produced by the pressure fluctuations. These fields can also lead, owing to the orientation of the anisotropic molecules (the quadratic Kerr effect), to an increase in the orientational inhomogeneities and, for example as a result of the electrocaloric effect, to an increase of the temperature inhomogeneities in the medium.

All three foregoing effects, on which the stimulated molecular scattering of light is based, are quadratic in the field, and as a result of the mixing of the exciting and scattered light waves, which differ in frequency and in wave number, the action of the light will affect primarily those Fourier components of the fluctuations which have caused the initial thermal scattering. The already mentioned increase of the inhomogeneities in the medium leads in turn to an increase in the intensity of the scattered light, which causes an increase in the inhomogeneities, etc. The intensity of the scattered light will grow nonlinearly as the light propagates in the region of the nonlinear interaction between the light and the medium.

Thus, the action of light on a medium leads to a change in the dielectric constant of the medium by an amount $\Delta\epsilon$, and consequently an additional nonlinear

*In order to distinguish thermal scattering of light from stimulated scattering, we use this term rather than the term "spontaneous scattering," since molecular scattering of light is always a stimulated rather than spontaneous process.

polarization of the medium appears:

$$\mathcal{P}^{nl}=\frac{\Delta\varepsilon}{4\pi}\mathbf{E}=\frac{1}{4\pi}\left[\left(\frac{\partial\varepsilon}{\partial p}\right)_{S,\zeta}p+\left(\frac{\partial\varepsilon}{\partial S}\right)_{p,\zeta}S+\left(\frac{\partial\varepsilon}{\partial\zeta}\right)_{p,S}\zeta\right]\mathbf{E};\quad(3)$$

here $\mathbf{E}$ is the total intensity of the electric field of the exciting and scattered light waves, and p, S, and ζ are the deviations of the pressure, entropy, and degree of orientation of the molecules from their equilibrium values. In (3) it is assumed that the change of ϵ occurs as a result of a change in pressure, entropy, and anisotropy of the medium, and when ϵ is expanded in terms of these parameters we can confine ourselves to the first term (weak nonlinearity). From Maxwell's equations, with allowance for the nonlinear addition to the polarization of the medium (3), we obtain

$$\tilde{\epsilon}\frac{\partial^2\mathbf{E}}{\partial t^2}+c^2\,\mathrm{rot}\,\mathrm{rot}\,\mathbf{E}=-\frac{\partial^2}{\partial t^2}\left[\left(\frac{\partial\varepsilon}{\partial p}\right)_{S,\zeta}p\mathbf{E}+\left(\frac{\partial\varepsilon}{\partial S}\right)_{p,\zeta}S\mathbf{E}+\left(\frac{\partial\varepsilon}{\partial\zeta}\right)_{p,S}\zeta\mathbf{E}\right],\quad(4)$$

where $\tilde{\epsilon}=\epsilon-i\epsilon''$ is the complex dielectric constant of the medium*. To solve the problem of stimulated molecular scattering we need also equations that describe the influence of the light waves on p, S, and ζ as a result of the indicated effects of striction, the electrocaloric effect, and the orientation of the molecules. In Ch. II, which is devoted to the theory of stimulated Mandel'shtam-Brillouin scattering (SMBS), we shall consider this equation for p and approximate solutions of this equation (together with the nonlinear Maxwell's equation). In Ch. III we describe the results of an experimental study of SMBS and where possible compare experiment with theory. In Ch. IV we describe the theory and experimental results for STS. The stimulated Rayleigh-wing scattering calls for a special review.

II. THEORY OF STIMULATED MANDEL'SHTAM-BRILLOUIN SCATTERING

The question of SMBS was considered theoretically in many papers[3,5,13-21,121]. Our exposition of the theory is based principally on the results of the nonstationary linear theory of Kroll[19] and the stationary nonlinear theory of Tang[20], which present the basic and various features of this phenomenon.

1. Initial Equations

Propagation of light waves with total electric-field intensity $\mathbf{E}$ produces in a medium electrostriction forces, with a volume density[22]

$$\mathbf{f}=\frac{1}{8\pi}\,\mathrm{grad}\left[\mathbf{E}^2\left(\rho\frac{\partial\varepsilon}{\partial\rho}\right)_T\right]-\frac{\mathbf{E}^2}{8\pi}\,\mathrm{grad}\,\varepsilon.\quad(5)$$

For the relative change in density $u=\rho_1/\rho$ we obtain from the hydrodynamic theory the following equation[23]:

$$\frac{\partial^2u}{\partial t^2}-\nabla^2\left(v_p^2u+\Gamma\frac{\partial u}{\partial t}\right)=-\frac{1}{\rho}\,\mathrm{div}\,\mathbf{f},\quad(6)$$

where v_p is the phase velocity of the sound in the medium in the absence of an electric field, $\Gamma=(\eta'+(4/3)\eta)/\rho$, and η' and η are the bulk and shear viscosity coefficients.

Substituting (5) in (6), neglecting small terms (of higher order in the field than $\mathbf{E}^2$) in the right side of (6), and making the substitution $u=(1/\rho)(\partial\rho/\partial p)p$, we obtain for the pressure p in the medium the following equation:

$$\frac{\partial^2p}{\partial t^2}=\nabla^2\left(v^2p+\Gamma\frac{\partial p}{\partial t}-\frac{Y}{8\pi\rho\beta_S}\mathbf{E}^2\right).\quad(7)$$

In (7) we have introduced the notation

$$\beta_S=\frac{1}{\rho v^2},\qquad Y=\rho\left(\frac{\partial\varepsilon}{\partial\rho}\right)_S,\quad(8)$$

$$v^2=v_p^2+\frac{1}{8\pi}\frac{\partial\varepsilon}{\partial\rho}|\mathbf{E}|^2,\quad(9)$$

where β_S is the compressibility of the medium, and Y is the parameter of nonlinear coupling, taken at constant S because we shall consider below hypersound frequencies ($\sim10^9$–10^{10} Hz), when the processes under consideration are adiabatic.

The sound velocity v is generally speaking a function of the amplitude of the electric field of the strong electromagnetic wave. But since p is of the order $|\mathbf{E}|^2$, it is clear from (7) that allowance for the field-independent correction in (9) is connected with a higher approximation than is used here.

We shall assume that the SMBS phenomenon develops independently of the remaining nonlinear processes. Then there remains in the right side of (4) only a term containing the pressure p; recognizing that the correction connected with allowance for the transversality of the light wave is small (div $\mathbf{D}=0$, and consequently curl curl $\mathbf{E}=-(1/n^2)Y\beta_S\nabla(\nabla p\mathbf{E})-\nabla^2\mathbf{E}\approx-\nabla^2\mathbf{E}$), we obtain the equation

$$\frac{n^2}{c^2}\frac{\partial^2\mathbf{E}}{\partial t^2}-\nabla^2\mathbf{E}-2i\frac{k_\omega n}{\omega c}\frac{\partial^2\mathbf{E}}{\partial t^2}=-\frac{1}{c^2}Y\beta_S\frac{\partial^2(p\mathbf{E})}{\partial t^2},\quad(10)$$

where $2k_\omega=\omega_0\epsilon''/cn$ is the extinction coefficient of the light, and $c=c_0/n$ is the velocity of the light in the medium.

The system (7) and (10) is the starting point for the solution of the SMBS problem. We seek the solution in the form of plane waves with slowly varying amplitudes

$$\mathbf{E}=\frac{1}{2}\sum_{l=0}^{2}\mathbf{E}_l(t,\mathbf{r})\exp(i\omega_lt-i\mathbf{k}_l\mathbf{r})+\text{c.c.}\quad(11)$$

$$p=\frac{1}{2}p(t,\mathbf{r})\exp(i\Omega t-i\mathbf{q}\mathbf{r})+\text{c.c.}\quad(12)$$

In (11), ω_0, $\mathbf{k}_0$, and $\mathbf{E}_0$ pertain to the exciting light wave, while ω_1, $\mathbf{k}_1$, $\mathbf{E}_1$ and ω_2, $\mathbf{k}_2$, $\mathbf{E}_2$ pertain to the scattered Stokes and anti-Stokes light waves. We assume further than

$$\omega_0=\omega_1+\Omega=\omega_2-\Omega,\quad\Delta_1=\mathbf{q}-\mathbf{k}_0+\mathbf{k}_1,\quad\Delta_2=\mathbf{q}+\mathbf{k}_0-\mathbf{k}_2.\quad(13)$$

It is obvious that the conditions $\Delta_1=\Delta_2=0$ correspond to the Bragg condition for the interaction of optical and acoustic waves, and the difference between these quantities and zero leads to a definite detuning. Finally, we assume that the amplitudes of the light and acoustic waves vary slowly compared with the oscillations of these waves, i.e., the following conditions are satisfied

$$|\mathbf{k}_l|,\ |\mathbf{q}|\gg\left|\frac{1}{E_l}\frac{\partial E_l}{\partial x}\right|,\quad\left|\frac{1}{p}\frac{\partial p}{\partial x}\right|,\quad\omega_l,\ \Omega\gg\left|\frac{1}{E_l}\frac{\partial E_l}{\partial t}\right|,\quad\left|\frac{1}{p}\frac{\partial p}{\partial t}\right|.\quad(14)$$

Substituting (11) and (12) in (7) and (10), neglecting (as a result of the condition (14)) the second derivatives of the amplitudes, and equating the expressions for the corresponding exponentials, we obtain for the interacting waves with amplitudes $\mathbf{E}_0$, $\mathbf{E}_1$, $\mathbf{E}_3$ and for p the following system of equations:

*It is assumed here that $\epsilon''\ll\epsilon$.

$$\frac{\omega_0 n^2}{c^2}\frac{\partial \mathbf{E}_0}{\partial t}+(\mathbf{k}_0\nabla)\mathbf{E}_0-\frac{1}{2}i\left(\mathbf{k}_0^2-\frac{\omega_0^2 n^2}{c^2}\right)\mathbf{E}_0+k_\omega|\mathbf{k}_0|\mathbf{E}_0 \quad (15a)$$

$$=-\frac{i\omega_0^2}{4c^2}\gamma\beta_S\{pE_1e^{-i\Delta_1 r}+p^*E_2e^{i\Delta_2 r}\}, \quad (15b)$$

$$\frac{\omega_1 n^2}{c^2}\frac{\partial \mathbf{E}_1}{\partial t}+(\mathbf{k}_1\nabla)\mathbf{E}_1-\frac{1}{2}i\left(\mathbf{k}_1^2-\frac{\omega_1^2 n^2}{c^2}\right)\mathbf{E}_1+k_\omega|\mathbf{k}_1|\mathbf{E}_1=$$

$$=-\frac{i\omega_1^2}{4c^2}\gamma\beta_S\mathbf{E}_0p^*e^{i\Delta_1 r},$$

$$\frac{\omega_2 n^2}{c^2}\frac{\partial \mathbf{E}_2}{\partial t}+(\mathbf{k}_2\nabla)\mathbf{E}_2-\frac{1}{2}i\left(\mathbf{k}_2^2-\frac{\omega_2^2 n^2}{c^2}\right)\mathbf{E}_2+k_\omega|\mathbf{k}_2|\mathbf{E}_2$$

$$=-\frac{i\omega_2^2}{4c^2}\gamma\beta_S\mathbf{E}_0pe^{-i\Delta_2 r}, \quad (15c)$$

$$\frac{\Omega}{v^2}\frac{\partial p}{\partial t}+(\mathbf{q}\nabla)p-\frac{1}{2}i\left(\mathbf{q}^2-\frac{\Omega^2}{c^2}\right)p+\alpha|\mathbf{q}|p$$

$$=-\frac{i\gamma}{16\pi}\{\mathbf{E}_0\mathbf{E}_1^*(\mathbf{q}-\Delta_1)^2e^{i\Delta_1 r}+\mathbf{E}_0^*\mathbf{E}_2(\mathbf{q}-\Delta_2)^2e^{i\Delta_2 r}\}. \quad (15d)$$

The last equation was obtained under the assumption $\Gamma\Omega/v^2 = \alpha\Lambda/\pi \ll 1$ (the condition for the existence of acoustic waves), where $\alpha = \Gamma q^2/2v$ is the amplitude coefficient of sound attenuation. The system (15) cannot be solved analytically in general form.

We continue the study of the SMBS phenomenon by analyzing the system (15) under various additional limiting assumptions. An analysis shows that at not too small scattering angles the anti-Stokes component does not become amplified as a result of the nonlinear interaction but attenuates, and therefore will be disregarded in this chapter. As to small scattering angles, the situation there is different, and we shall return to this question later.

2. Linear Nonstationary Theory

We assume that the Bragg condition is satisfied, i.e., that $\Delta_1 = \Delta_2 = 0$. This means that the shift of the Mandel'shtam-Brillouin components Ω_{MB} relative to the frequency of the exciting light is determined by the expression (1). We put further $\mathbf{k}_l^2 = n^2\omega_l^2/c^2$, $\mathbf{q}^2 = \Omega^2/v^2$, and $|\mathbf{E}_0| \gg |\mathbf{E}_1|, |\mathbf{E}_2|$, $|\mathbf{E}_0|^2 = \text{const}$ (the approximation of a given exciting wave). Then, neglecting the anti-Stokes scattering, we obtain from (15) the following linearized system of equations for the amplitudes of the Stokes optical and hypersonic waves:

$$\frac{\omega_1^2 n^2}{c^2}\frac{\partial \mathbf{E}_1}{\partial t}+(\mathbf{k}_1\nabla)\mathbf{E}_1+k_\omega|\mathbf{k}_1|\mathbf{E}_1=-\frac{i\omega_1^2}{4c^2}\gamma\beta_S\mathbf{E}_0p^*,$$

$$\frac{\Omega}{v^2}\frac{\partial p^*}{\partial t}+\mathbf{q}\nabla p^*+\alpha|\mathbf{q}|p^*=\frac{iq^2}{16\pi}\mathbf{E}_0^*\mathbf{E}_1. \quad (16)$$

The system (16) has exponential solutions, from which, generally speaking, it is possible to construct a general solution if the initial and boundary conditions are specified. In the general case of scattering at an arbitrary angle, this problem is quite complicated. It is a relatively simple matter to analyze SMBS in two particular but important cases: a) the case of SMBS in a resonator, when the scattering direction (k_1) is set by the resonator axis, and b) backward scattering ($\vartheta = 180°$).

a) SMBS in a resonator. For the case of a resonator, we seek the solution of (16) in the form* $E_1 \sim p^* \sim \exp(\beta t + i\mathbf{b}\cdot\mathbf{r})$. Inserting these expressions in (16), we obtain a dispersion relation from which, recognizing that $v/c \ll 1$, we obtain the following expression for β:

$$\beta_{1,2}=\frac{1}{2}\left(-\alpha v-\frac{1}{n}k_\omega c-\frac{1}{n}ic\frac{\mathbf{k}_1\mathbf{b}}{|\mathbf{k}_1|}\right)$$

$$\pm\frac{1}{2}\left\{\left(\alpha v-\frac{1}{n}k_\omega c-\frac{1}{n}ic\frac{\mathbf{k}_1\mathbf{b}}{|\mathbf{k}_1|}\right)^2+\frac{\omega_1\Omega\gamma^2\beta_S}{16\pi n^2}|\mathbf{E}_0|^2\right\}^{1/2}. \quad (17)$$

*The oscillating spatial variation is chosen to satisfy the boundary conditions in the resonator.

It is seen from (17) that only one solution (Re $\beta_1 > 0$) corresponds to an increase of the amplitude of the field of the scattered wave and the hypersound wave with time (temporal instability). The maximum value of β occurs at $b = 0$, and the threshold for the occurrence of SMBS generation in the resonator is determined by the condition Re $\beta_1 \geq 0$, or

$$\frac{|\mathbf{E}_0|^2}{8\pi}\geqslant\left(\frac{|\mathbf{E}_0|^2}{8\pi}\right)_{\text{thr}}=\frac{8n^2k_\omega\alpha}{\gamma^2\beta_S|\mathbf{q}||\mathbf{k}_1|}. \quad (18)$$

When the threshold is greatly exceeded, neglecting in (17) the acoustic and optical losses, we obtain

$$\beta\approx\frac{\gamma|\mathbf{E}_0|}{8n}\left(\frac{\omega_1\Omega\beta_S}{\pi}\right)^{1/2}, \quad (19)$$

and near the threshold we get from the expansion (17)

$$\beta\approx\frac{c}{n}\left(-k_\omega+\frac{|\mathbf{q}||\mathbf{k}_1|\gamma^2\beta_S}{64\pi n^2\alpha}|\mathbf{E}_0|^2\right). \quad (20)$$

Substituting in (16) the solution for p and E_1 in the indicated exponential form, we find that near the threshold the ratio of the energy density of the scattered wave, W_1, to the energy density in the acoustic wave, W_p, is given by

$$\frac{W_1}{W_p}\approx\frac{\omega_1\alpha\gamma n}{\Omega k_\omega c}. \quad (21)$$

and in the case of an appreciable excess over threshold

$$\frac{W_1}{W_p}\approx\frac{\omega_1}{\Omega}. \quad (22)$$

The latter equation (the Manley-Rowe relation) means that in the SMBS process the creation of each photon is accompanied by the creation of a phonon.

b) Backward scattering (scattering angle $\vartheta = 180°$). In this case the solution of the system (16) is sought in the form $E_1 \sim p^* \sim \exp(i\beta t + bx)$. We shall assume that $\mathbf{E}_1$ propagates in the positive x direction. As in the preceding case, we obtain the dispersion relation and, reocgnizing that $v/c \ll 1$, we obtain

$$b_{1,2}=\frac{1}{2}\left(-\alpha-k_\omega+i\frac{\beta}{v}\right)\pm\frac{1}{2}\left\{\left(\alpha+k_\omega+i\frac{b}{v}\right)^2-\frac{|\mathbf{q}||\mathbf{k}_1|\gamma^2\beta_S}{16\pi n^2}|\mathbf{E}_0|^2\right\}^{1/2}. \quad (23)$$

The boundary conditions are specified in the form:

$$E_1(0,t)=E_{10}\exp(i\beta t), \qquad p^*(L,t)=0. \quad (24)$$

Taking (23) and (24) into account, we obtain from (16) for $E_1(x, t)$

$$E_1(x,t)=E_{10}\exp(i\beta t+b_2x)\cdot\frac{1-\frac{k_\omega+b_2}{k_\omega+b_1}\exp\{(b_2-b_1)(L-x)\}}{1-\frac{k_\omega+b_2}{k_\omega+b_1}\exp\{(b_2-b_1)L\}}. \quad (25)$$

The signs of b_1 and b_2 in (23) are chosen such as to make Re $(b_2 - b_1) \leq 0$.

In sufficiently weak fields, when $|\mathbf{E}_0|^2 < (|\mathbf{E}_0|^2)_{cr}$ (an expression for $(|\mathbf{E}_0|^2)_{cr}$ is given below), the gain is stable in the entire region of interaction, and as $L \to \infty$ it follows from (25) that

$$E_1=E_{10}\exp(i\beta t+b_2x). \quad (26)$$

The SMBS gain is maximal at $\beta = 0$ (stationary regime) and equals

$$g_{MB}=2b_2=\alpha-k_\omega-\left\{(\alpha+k_\omega)^2-\frac{1}{16\pi n^2}|\mathbf{q}||\mathbf{k}_1|\gamma^2\beta_S|\mathbf{E}_0|^2\right\}^{1/2}$$

$$\approx-2k_\omega+\frac{|\mathbf{q}||\mathbf{k}_1|\gamma^2\beta_S|\mathbf{E}_0|^2}{32\pi n^2\alpha}. \quad (27)$$

The latter approximate expression is obtained when $|\mathbf{E}_0|^2 \ll (|\mathbf{E}_0|^2)_{cr}$.

From (27) it is easy to find the condition under which the gain g_{MB} is positive. From the same condition follows an expression for the threshold of the SMBS. This expression coincides with the previously obtained expression (18), which determines the onset of generation of SMBS in a resonator.

Under certain conditions, temporal instability can develop in SMBS at an angle $\vartheta = 180°$. When $|\mathbf{E}_0|^2 > (|\mathbf{E}_0|^2)_{cr}$ or

$$\frac{|\mathbf{E}_0|^2}{8\pi} > \left(\frac{|\mathbf{E}_0|^2}{8\pi}\right)_{cr} = \frac{2n^2(\alpha+k_\omega)^2}{|\mathbf{q}|\,|\mathbf{k}_1|\,Y^2\beta_S} \tag{28}$$

there exists a critical length L_{cr} such that if $L \geq L_{cr}$ the regime becomes unstable and generation is possible. This follows from the fact that there exist real positive quantities $\beta' = i\beta$ for which the denominator in (25) vanishes. The condition under which the denominator in (25) vanishes can be written in the form

$$\left(\alpha+k_\omega+\frac{\beta'}{v}\right)\operatorname{tg}\left\{\frac{1}{2}L_{cr}\left[\frac{|\mathbf{q}|\,|\mathbf{k}_1|\,Y^2\beta_S}{16\pi n^2}|\mathbf{E}_0|^2-\left(\alpha+k_\omega+\frac{\beta'}{v}\right)^2\right]^{1/2}\right\} = -\left[\frac{|\mathbf{q}|\,|\mathbf{k}_1|\,Y^2\beta_S}{16\pi n^2}|\mathbf{E}_0|^2-\left(\alpha+k_\omega+\frac{\beta'}{v}\right)^2\right]^{1/2}, \tag{29}$$

from which follows an inequality for the smallest value of L_{cr}:

$$\left(\frac{|\mathbf{q}|\,|\mathbf{k}_1|\,Y^2\beta_S|\mathbf{E}_0|^2}{16\pi n^2}-\frac{4\pi^2}{L_{cr}^2}\right)^{1/2} - (\alpha+k_\omega) < \frac{\beta'}{v} < \left(\frac{|\mathbf{q}|\,|\mathbf{k}_1|\,Y^2\beta_S|\mathbf{E}_0|^2}{16\pi n^2}-\frac{\pi^2}{L_{cr}^2}\right)^{1/2}-(\alpha+k_\omega). \tag{30}$$

When $L \to \infty$ we have

$$\frac{\beta'}{v} \to \left(\frac{|\mathbf{q}|\,|\mathbf{k}_1|\,Y^2\beta_S|\mathbf{E}_0|^2}{16\pi n^2}\right)^{1/2}-(\alpha+k_\omega),$$

and for $b_1 = b_2 = b$ we get

$$b = -k_\omega+\frac{1}{2}\left(\frac{|\mathbf{q}|\,|\mathbf{k}_1|\,Y^2\beta_S}{16\pi n^2}|\mathbf{E}_0|^2\right)^{1/2}. \tag{31}$$

The exponential dependence of the field amplitude in the unstable case takes the form

$$E_1 \sim \exp\left\{vt\left[\left(\frac{|\mathbf{q}|\,|\mathbf{k}_1|\,Y^2\beta_S}{16\pi n^2}|\mathbf{E}_0|^2\right)^{1/2}-(\alpha+k_\omega)\right] + x\left[\frac{1}{2}\left(\frac{|\mathbf{q}|\,|\mathbf{k}_1|\,Y^2\beta_S}{16\pi n^2}|\mathbf{E}_0|^2\right)^{1/2}-k_\omega\right]\right\}. \tag{32}$$

We note that the temporal instability (generation) develops at much higher light intensities than the stable exponential SMBS gain. Thus, from a comparison of (18) and (28) we obtain (when $k_\omega \ll \alpha$)

$$\frac{(|\mathbf{E}_0|^2)_{dir}}{(|\mathbf{E}_0|^2)_{cr}} \approx 4\frac{k_\omega}{\alpha}. \tag{33}$$

For pure liquids, (33) yields a value $\sim 10^{-6}$. From a comparison of (19) with (32) we can easily see that the rate of time growth of the field is larger by a factor $(c/v)^{1/2}/2$ in a resonator than in the development of temporal instability in the case of backward scattering. It should also be noted that the development of instability in backward scattering differs from temporal instability in a resonator. In the former case there is a spatial growth of the amplitude of the scattered wave, which dominates over the temporal growth when $x \gg vt$, while in the latter case the amplitudes only grow in time.

c) Transient time-dependent solutions. In items a) and b) we considered two particular cases of exponential solutions of the system of equations (16) for SMBS in a resonator and for SMBS at an angle $\vartheta = 180°$. We now consider the general case of time-dependent transient solutions for amplitudes in SMBS. To this end, we reduce the system of equations (16) to a more symmetrical form, introducing the notation

$$\nabla' = \frac{\partial}{\partial\boldsymbol{\xi}'}, \quad \boldsymbol{\xi}' = \frac{\mathbf{r}}{X}, \quad \tau = \frac{t}{T}, \quad \mathcal{P} = -i\left(\frac{4\pi|\mathbf{k}_1|\,\beta_S}{n^2|\mathbf{q}|}\right)^{1/2}p^*,$$

$$T = \frac{X}{v}, \quad \delta_3 = \alpha X, \quad \delta_1 = k_\omega X, \quad X = \left(\frac{64\pi n^2}{Y^2\beta_S|\mathbf{q}||\mathbf{k}_1||\mathbf{E}_0|^2}\right)^{1/2}, \quad \Psi = \frac{\mathbf{k}_1\mathbf{q}}{|\mathbf{k}_1||\mathbf{q}|}. \tag{34}$$

We consider the variation of the amplitudes along $\mathbf{k}_1$ and introduce a coordinate in this direction, $\xi = \mathbf{k}_1\boldsymbol{\xi}'/|\mathbf{k}_1|$. Then, taking (34) into account, we obtain from the system (16)

$$\frac{v}{c}\frac{\partial E_1}{\partial\tau}+\frac{\partial E_1}{\partial\xi}+\delta_1E_1 = \mathcal{P}, \qquad \frac{\partial\mathcal{P}}{\partial\tau}+\Psi\frac{\partial\mathcal{P}}{\partial\xi}+\delta_3\mathcal{P} = E_1. \tag{35}$$

The initial and boundary conditions are written as follows:

$$E_1(\xi, 0) = E_{10}\exp(-\delta_1\xi), \quad E_1(0, \tau) = E_{10}, \quad \mathcal{P}(\xi, 0) = \mathcal{P}_0, \quad \mathcal{P}(0, \tau) = \mathcal{P}_0\exp(-\delta_3\tau), \tag{36}$$

or

$$\mathcal{P}(\mathscr{L}, \tau) = \mathcal{P}_0\exp(-\delta_3\tau). \tag{37}$$

The last two conditions correspond either to forward scattering or to backwards scattering. From (35), (36), and (37), assuming that the condition $\xi \gg \tau$ ($x \gg vt$) is satisfied for $\Psi > 0$ and the condition $\xi < \mathscr{L} - \tau$ ($x < L - vt$) is satisfied for $\Psi < 0$, we get

$$E_1(\xi, \tau) = E_{10}e^{-\delta_1\xi} + \mathcal{P}_0\frac{1-e^{-\delta_1\xi}}{\delta_1}+\int_0^\xi\int_0^\tau E_1(\xi-\Psi\tau_1, \tau-\tau_1)e^{\delta_1(\xi_1-\xi)-\delta_3\tau}\,d\xi_1\,d\tau_1. \tag{38}$$

It is convenient to express the solution of (38) in terms of the function $U(\xi, \tau)$:

$$E_1(\xi, \tau) = E_{10}e^{-\delta_1\xi}U(\xi, \tau)+\mathcal{P}_0e^{-\delta_1\xi}\frac{\partial U(\xi, \tau)}{\partial\tau}, \tag{39}$$

where $U(\xi, \tau)$ satisfies the following integral equation:

$$U(\xi, \tau) = 1+\int_0^\tau\int_0^\xi U(\xi-\Psi\tau_1, \tau-\tau_1)e^{\delta_1\xi_1-\delta_3\tau_1}\,d\xi_1\,d\tau_1. \tag{40}$$

The solution of Eq. (40) is of the form

$$U(\xi, \tau) = 1+\xi\int_0^\tau\frac{\exp[(-\delta_3-\Psi\delta_1)\tau_1]}{\tau_1^{1/2}(\xi-\Psi\tau_1)^{1/2}}I_1[2\tau_1^{1/2}(\xi-\Psi\tau_1)^{1/2}]\,d\tau_1. \tag{41}$$

In (41), I_1 is a modified Bessel function of first order, the asymptotic value of which at large arguments is equal to

$$I_1[2\tau_1^{1/2}(\xi-\Psi\tau_1)^{1/2}] \approx \frac{\exp[2\tau_1^{1/2}(\xi-\Psi\tau_1)^{1/2}]}{[4\pi\tau_1^{1/2}(\xi-\Psi\tau_1)^{1/2}]^{1/2}}. \tag{42}$$

Substituting (42) in (41) and by the same token excluding the region of small ξ, we obtain for small values of τ_1

$$U(\xi, \tau) = 1+\frac{\xi}{(4\pi)^{1/2}}\int_0^\tau\frac{d\tau_1\exp[2\tau_1^{1/2}(\xi-\Psi\tau_1)^{1/2}-(\delta_3-\Psi\delta_1)\tau_1]}{[\tau_1(\xi-\Psi\tau_1)]^{3/4}}. \tag{43}$$

It is seen from (43) that in the case of backwards scattering ($\Psi < 0$) and if $(\delta_3 + \delta_1) < 2$, which coincides with the condition (28) for instability development, the integral (43) diverges when $\tau \to \infty$, and consequently the solution is unstable. In the case when the numerator under the integral sign in (43) has a maximum in the region from zero to τ, the approximate value of the integral (43) is

$$U(\xi, \tau) = \frac{\xi\exp[2\tau^{1/2}(\xi-\Psi\tau)^{1/2}-(\delta_3-\Psi\delta_1)\tau]}{(4\pi)^{1/2}[\tau(\xi-\Psi\tau)]^{1/4}[\xi-2\Psi\tau-(\delta_3-\Psi\delta_1)\tau^{1/2}(\xi-\Psi\tau)^{1/2}]}. \tag{44}$$

It is necessary here to satisfy the condition $\tau \gg 1$. In the stable case it is necessary, in addition, to satisfy the condition

$$\tau > \tau_{max} = \frac{\xi}{2\Psi}\left\{1 - \frac{(\delta_3 - \Psi\delta_1)}{[(\delta_3 - \Psi\delta_1)^2 + 4\Psi]^{1/2}}\right\}. \quad (45)$$

τ_{max} is that value of τ at which the numerator under the integral sign in (43) assumes its maximal value, and thus, when $\tau > \tau_{max}$ (and $\Psi > -(\delta_3 - \Psi\delta_1)/2$), a stationary regime is reached. Satisfaction of the condition (43) signifies that the maximum value of the numerator under the integral sign in (43) lies in the integration region. From (44) it follows that in the unstable case, in the case of backwards scattering ($\Psi = -1$, $\delta_3 + \delta_1 < 2$) and when $\tau \ll \xi$, in accord with (32), the exponential is of the form $\exp[(2 - \delta_3 - \delta_1)\tau + (1 - \delta_1)\xi]$. For the case of short pulses ($\tau \ll \xi$), assuming $\delta_1 \ll \delta_3$, we obtain from (44)

$$U(\xi, \tau) \sim \exp(2\tau^{1/2}\xi^{1/2} - \delta_3\tau). \quad (46)$$

In the case of stable amplification it is easy to obtain from (43), as $\tau \to \infty$ and with account taken of (45), in full agreement with the exponential solutions considered in item b)

$$\underset{\tau\to\infty}{U(\xi, \tau)} \to \exp\frac{\xi}{2\Psi}\{-(\delta_3 - \Psi\delta_1) + [(\delta_3 - \Psi\delta_1)^2 + 4\Psi]^{1/2}\}. \quad (47)$$

Thus, the variation of $E_1(\xi, \tau)$ is determined mainly by the exponential (44) or (47) which, according to (39), must also be multiplied by $\exp(-\delta_1\xi)$.

So far we have specified through the initial values of p_0 and E_{10} on the boundary; consequently, for example for the stable case at large values of t, the source should vanish. Actually, in SMBS we should start from the fact that the sources p_0 and E_{10} are of fluctuation origin, and on the average they are uniformly distributed in the medium. We neglect the spontaneous fluctuations of the electromagnetic field and see how account can be taken of the uniform distribution of the thermal sources of pressure in the wave-interaction region. Assume that the medium contains N sources that are excited at arbitrary randomly distributed instants of time τ_i and with random amplitudes $\mathcal{P}_i$. We can then write for the medium

$$\mathcal{P}_T = \sum_i \mathcal{P}_i\Theta(\tau - \tau_i)\exp[(\tau_i - \tau)\delta_3], \quad (48)$$

where $\Theta(\tau) = 1$ for $\tau > 0$ and $\Theta(\tau) = 0$ for $\tau < 0$. The mean value over the ensemble is

$$\langle\mathcal{P}_T^2\rangle = N\langle\mathcal{P}_i^2\rangle\int_{-\infty}^{\tau}\exp[2\delta_3(\tau_i - \tau)]\,d\tau_i, \quad (49)$$

or $2\delta_3\langle\mathcal{P}_T^2\rangle = N\langle\mathcal{P}_i^2\rangle$. On the basis of (39) we can write for E_1

$$E_1(\xi, \tau) = \sum_{i,\ \tau_i<0}\mathcal{P}_i\dot{U}(\xi, \tau)\exp(\delta_3\tau_i) + \sum_{i,\ \xi>\tau_i>0}\mathcal{P}_i\dot{U}(\xi, \tau - \tau_i).$$

After averaging we obtain

$$\langle E_1^2(\xi, \tau)\rangle = \langle\mathcal{P}_T^2\rangle\left\{[\dot{U}(\xi, \tau)]^2 + 2\delta_3\int_0^{\tau}d\tau_1[\dot{U}(\xi, \tau_1)]^2\right\}. \quad (50)$$

Replacing $\mathcal{P}$ by p, we obtain the following dependence of the intensity $\mathcal{J}_1$ of the scattered wave on the intensity $\mathcal{J}_T$ of the thermal fluctuations of pressure (the intensity of the Debye waves):

$$\mathcal{J}_1 = \frac{\omega_1}{\Omega}\mathcal{J}_T\left\{[\dot{U}(\xi, \tau)]^2 + 2\delta_3\int_0^{\tau}d\tau_1[\dot{U}(\xi, \tau_1)]^2\right\}. \quad (51)$$

$\mathcal{J}_T$ can be easily calculated by the methods of statistical physics. In the same manner as used to derive (51), we can obtain, using the first equation of the system (35) and neglecting the optical losses, the connection between the intensity $\mathcal{J}_1$ of the scattered light wave and the intensity $\mathcal{J}_p$ of the sound wave in SMBS:

$$\frac{\mathcal{J}_p}{\mathcal{J}_1} = \left(\frac{\Omega}{\omega_1}\right)\left[\left(\frac{\partial\dot{U}}{\partial\xi}\right)^2 + 2\delta_3\int_0^{\tau}d\tau_1\left(\frac{\partial\dot{U}}{\partial\xi}\right)^2\right]\Big/\left[\dot{U}^2 + 2\delta_3\int_0^{\tau}d\tau_1[\dot{U}]^2\right]. \quad (52)$$

For short pulses, using (46), we obtain

$$\frac{\mathcal{J}_p}{\mathcal{J}_1} = \frac{\Omega}{\omega_1}\frac{\tau}{\xi} = \frac{\Omega}{\omega_1}\frac{vt}{x} \qquad (vt \ll x). \quad (53)$$

Consequently, the intensity of the sound wave for short pulses will be much shorter than follows from the Manley-Rowe relation.

3. Stationary Theory of SMBS

For a medium with sufficiently large acoustic losses, when the instability cannot develop and the laser pulse duration is much larger than the phonon lifetime, we can consider a stationary problem. The requirement that the pulse duration t_0 be much larger than the lifetime of the phonons $\tau_{ph} = 1/2\alpha v$, means, in other words, that the spectral width of the laser radiation $\delta\omega_0$ should be much smaller than the line width of the thermal Mandel'shtam-Brillouin scattering, owing to the finite duration of the pulse, i.e., $\delta\omega_0 \ll \delta\Omega_{MB}$. More accurately speaking, the time of attenuation of the transient time-dependent solutions is determined by expression (45), from which it follows that far from the instability region ($\delta_3 \gg 2$) the stationary state is reached at pulse durations

$$t_0 > \tau_{MB}L/2\alpha v = \tau_{ph}J, \quad (54)$$

where g_{MB} is the gain in the case of stable SMBS, and $J = g_{MB}L$ is the gain in the entire region of nonlinear interaction.

Let us examine, following[20], the most interesting case of backward scattering, in which account can also be taken of the saturation effect, when the intensity of the scattered light can become comparable with the intensity of the exciting light (nonlinear solutions). In the stationary problem it is also possible to trace the variation of the width of the SMBS components. To this end it is necessary to take into account the possibility of incomplete synchronism, i.e., to assume $\Delta_1 \neq 0$ in the general system of equations (15). Then, recognizing that the exciting light and the sound wave propagate forward, while the scattered light propagates backwards (towards decreasing x), we obtain

$$\left.\begin{aligned} &\frac{\partial E_0}{\partial x} + k_0E_0 = -\frac{i\omega_0}{4c}Y\beta_S pE_1e^{-i\chi\Delta}, \quad \frac{\partial p}{\partial x} + \alpha p = -\frac{i|\mathbf{q}|}{16\pi}E_0E_1^*e^{i\chi\Delta};\\ &-\frac{\partial E_1}{\partial x} + k_0E_1 = -\frac{i\omega_1}{4c}Y\beta_S p^*E_0e^{i\chi\Delta}, \end{aligned}\right\} \quad (55)$$

here $\Delta = q - k_0 - k_1 \approx (1/v)(\overline{\omega}_1 - \omega_1)$, where $\overline{\omega}_1 = \omega_0[1 - (2n\,2v/c)]$ is the ordinary Stokes frequency when the Bragg condition is satisfied ($\vartheta = 180^\circ$). Putting $\omega_1 \neq \overline{\omega}_1$, we consider by the same token a finite amplification band. In the general case, the system (55) can-

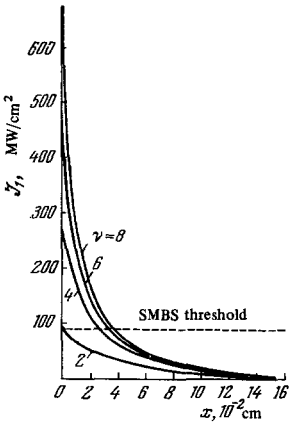

FIG. 1

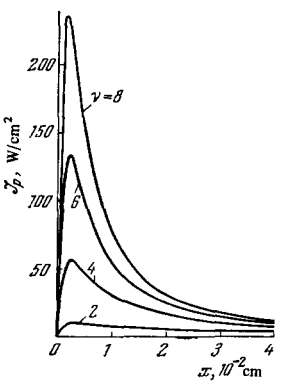

FIG. 2

FIG. 1. Intensity of SMBS in CS_2 as a function of the distance from the start of the region of nonlinear interaction for several values of $\mathcal{J}_0 = \nu\mathcal{J}_{thr}$ ($\mathcal{J}_{thr} = 90$ MW/cm^2 - threshold intensity for CS_2, $\nu = 2, 4, 6, 8$) [21]. The following CS_2 parameters were used in the calculation: $\rho = 1.26$ g/cm^3, $n = 1.62$, $Y = 2.50$, $v = 1.24 \times 10^5$ cm/sec, $\alpha = 1600$ cm^{-1}.

FIG. 2. Intensity of hypersound in SMBS in CS_2 as a function of the distance from the start of the region of nonlinear interaction for several values of $\mathcal{J}_0 = \nu\mathcal{J}_{thr}$ ($\nu = 1, 4, 6, 8$) [21].

not be solved analytically*.

For the case of carbon disulfide, assuming that $k_\omega = \Delta = 0$ and $\alpha \neq 0$, the system (55) was solved numerically in[21]. The results of the calculations are shown in Figs. 1 and 2. The boundary conditions were as follows: $E_0(0) = E_0$ and $p(0) = 0$ at $x = 0$, and $E_1(L) = 0$ at $x = L$, where L is the value of x at which the intensity of the exciting light is decreased as a result of the SMBS to its threshold value $\mathcal{J}_{0thr}$, after which the SMBS stops. It is obivous that in this case the condition $|E_0|^2 = |E_1|^2 + (|E_0|^2)_{thr}$ should be satisfied.

Figure 1 shows the dependence of the intensity of the backward scattered Stokes radiation on the depth of penetration x of the exciting light in the medium at different values of the intensity of the latter (for each curve, the parameter is $\nu = \mathcal{J}_0(0)/\mathcal{J}_{0thr}$). It is seen from Fig. 1 that the main fraction of the scattered light is in the region $\sim 2 \times 10^{-2}$ cm.

Figure 2 shows the dependence of the hypersound intensity on the coordinate for different intensities $\mathcal{J}_0(0)$. The intensity of the hypersound reaches a maximum at a distance $x \approx (1-2) \times 10^{-3}$ cm from the entrance of the laser radiation. At large x, the decrease of p is connected both with the large absorption coefficient of the sound and with the decrease of the amplitudes E_1 and E_0. Let us consider the approximate solution of the system (55), when the phonon mean free path is much smaller than the region of the nonlinear interaction. From the last equation of (55) it follows that

$$p(x) = -\frac{i}{16\pi} Y |\mathbf{q}| \int_0^x E_0(x') E_1^*(x') e^{ix'\Delta - \alpha(x-x')}\, dx' + p(0)\, e^{-\alpha x}. \quad (56)$$

We take into account the fact that the factor $\exp\{-\alpha(x - x')\}$ makes the main contribution to (56) in the region $x' - x \leq 1/\alpha$, and assume that the rate of acoustic loss is larger than the rate of variation of E_0 and E_1 as a result of the SMBS, i.e., that

$$\alpha \gg \left|\frac{1}{E_0}\frac{\partial E_0}{\partial x}\right|, \left|\frac{1}{E_1}\frac{\partial E_1}{\partial x}\right|. \quad \text{B}$$

We can then take $E_0(x')E^*(x')$ in (56) outside the integral sign, and take this value at $x = x'$, i.e., we get

$$p = -\frac{iY|\mathbf{q}|E_0(x)E_1^*(x)}{16\pi(i\Delta+\alpha)} e^{ix\Delta} \quad \left(x \gg \frac{1}{\alpha}\right). \quad (57)$$

Consequently, the amplitude of the sound wave is proportional to the product of the local intensities of the exciting and scattered light waves. Since p is inversely proportional to the resonance factor $i\Delta + \alpha$, the pressure has a maximum at $\Delta = 0$, i.e., when the Bragg condition is exactly satisfied, and the gain occurs in the frequency interval $\delta\Omega = 2\alpha v$. Substituting (57) in the first and second equations of the system (55), we get

$$\frac{\partial E_0}{\partial x} + k_\omega E_0 = -\frac{|\mathbf{q}||\mathbf{k}_0|Y^2\beta_S|E_1|^2E_0}{64\pi n^2(i\Delta+\alpha)}, \quad \frac{\partial E_1}{\partial x} - k_\omega E_1 = \frac{|\mathbf{q}||\mathbf{k}_1|Y^2\beta_S|E_0|^2E_1}{64\pi n^2(i\Delta-\alpha)}. \quad (58)$$

We introduce the intensities of the exciting and scattered light waves

$$\mathcal{J}_0 = \frac{cn|E_0|^2}{8\pi} \quad \text{and} \quad \mathcal{J}_1 = \frac{cn|E_1|^2}{8\pi}.$$

We then obtain from (58), assuming that $\omega_0 - \omega_1 = \Omega \ll \omega_0$ and $|\mathbf{k}_0| \approx |\mathbf{k}_1| \approx |\mathbf{k}|$,

$$\frac{\partial\mathcal{J}_0}{\partial x} + 2k_\omega\mathcal{J}_0 = -G(\omega_1)\mathcal{J}_0\mathcal{J}_1, \quad \frac{\partial\mathcal{J}_1}{\partial x} - 2k_\omega\mathcal{J}_1 = -G(\omega_1)\mathcal{J}_0\mathcal{J}_1, \quad (59)$$

where

$$G(\omega_1) = \frac{|\mathbf{q}||\mathbf{k}_1|Y^2\beta_S}{4n^3c} \frac{\alpha v^2}{\alpha^2v^2 + (\omega_1 - \omega_1)^2}. \quad (60)$$

It is easy to obtain from (59) the threshold value $|E_0|^2_{thr}$, i.e., the condition under which the gain exceeds the loss. This is the condition $G(\omega_1)\mathcal{J}_0 > 2k_\omega$, which coincides when $\omega_1 = \omega_1$ with the previously obtained condition (18). In the linear approximation, when we can put $\mathcal{J}_0 \sim$ const, the gain g_{MB} and G are connected by the relation

$$g_{MB} = -2k_\omega + G(\omega_1)\mathcal{J}_0(0). \quad (61)$$

Usually $2k_\omega$ is a small quantity (smaller than 10^{-2} cm^{-1}) in the absence of nonlinear absorption and scattering effects. Therefore in the real case, far from the SMBS threshold, the optical loss can be neglected. Putting $k_\omega = 0$, we obtain the following solution for the system of nonlinear equations (59):

$$\left.\begin{aligned} \mathcal{J}_0(x) &= \mathcal{J}_1(x) + \mathcal{J}_0(0) - \mathcal{J}_1(0), \\ \mathcal{J}_1(0) &= \frac{\mathcal{J}_1(0)\left[1 - \frac{\mathcal{J}_1(0)}{\mathcal{J}_0(0)}\right]}{\exp\left\{\left[1 - \frac{\mathcal{J}_1(0)}{\mathcal{J}_0(0)}\right]G(\omega_1)\mathcal{J}_0(0)\,x\right\} - \frac{\mathcal{J}_1(0)}{\mathcal{J}_0(0)}}. \end{aligned}\right\} \quad (62)$$

As seen from (62), in the limit as $\mathcal{J}_1(0)/\mathcal{J}_0(0) \to 0$, we obtain an exponential growth of the Stokes SMBS component in space:

$$\mathcal{J}_1(0) = \mathcal{J}_1(x)\exp[G(\omega_1)\mathcal{J}_0(0)\,x]. \quad (63)$$

*In the particular case when $k_\omega = \alpha = 0$ and $\Delta = 0$, we can obtain exact analytic solutions of the system (55) in terms of elliptic Jacobi functions. These solutions were obtained in [24] and are given in [1]. They are not given here, since these solutions are not applicable to most real cases. In addition, it should be noted that when $\alpha \to 0$ it is necessary to consider the nonstationary problem, as follows from the linear nonstationary theory.

In (62), the unknown quantities are assumed to be $\mathcal{J}_1(1)$ (the initial intensity of the Stokes scattering) and $\mathcal{J}_0(x)$. The boundary conditions for $\mathcal{J}_0$ are specified at x = 0 and for $\mathcal{J}_1$ at x = L. Consequently, in order to use (62) it is necessary to calculate $\mathcal{J}_1(0)$ putting x = L. From the first equation of (62) it is easy to see that in the limit, when L increases, $\mathcal{J}_1(0)$ also increases monotonically and reaches the limit that is expected on the basis of the Manley-Rowe relation ($\mathcal{J}_1/\mathcal{J}_0 \approx \omega_1/\omega_0 \approx 1$):

$$\lim_{L\to\infty} \mathcal{J}_1(0) = \mathcal{J}_0(0) + \mathcal{J}_1(L).$$

As follows from the calculation of[20], the saturation effect due to the reaction of the intensity of the Stokes radiation on the intensity of the exciting radiation, comes into play when $\mathcal{J}_1(0)$ reaches several per cent of the intensity of the initial exciting radiation, regardless of whether this is a consequence of the large length of the interaction region or the large value of $\mathcal{J}_0(0)$. At saturation, the rate of growth of the SMBS intensity decreases, although it can remain exponential as before[20].

In the case under consideration, the intensity of the hypersound wave depends essentially on the sound attenuation coefficient. From (57) we can easily obtain for the intensity of the hypersound $\mathcal{J}_p(x)$

$$\mathcal{J}_p(x) = \left[\frac{G(\omega_1)\mathcal{J}_0(x)}{2\alpha}\right]\left[\frac{\Omega}{\omega_0}\mathcal{J}_1(x)\right]. \quad (64)$$

The intensity of the hypersound wave should reach its maximum value at $x \approx 1/\alpha$. Consequently, the maximum value of $\mathcal{J}_p(x)$ can be calculated from the relation

$$(\mathcal{J}_p)_{\max} \approx \mathcal{J}_p\left(\frac{1}{\alpha}\right) \approx \left[\frac{G(\omega_1)\mathcal{J}_0(0)}{2\alpha}\right]\left[\frac{\Omega}{\omega_0}\mathcal{J}_1(0)\right] = \frac{g_{MB}}{2\alpha}\frac{\Omega}{\omega_0}\mathcal{J}_1(0). \quad (65)$$

The first factor in (64) or (65) leads to a decreased value of the hypersound intensity compared with the value that follows from the Manley-Rowe relation (second factor). For liquids usually $2\alpha \sim 10^3-10^4$ cm^{-1} and even when $\mathcal{J}_1(0) \sim \mathcal{J}_0(0)$ (usually $g_{MB} \sim 10-10^2$ cm^{-1}) the intensity of the hypersound is much smaller than that calculated in accordance with Manley and Rowe. At the same time, as noted above, the Manley-Rowe relation is applicable to the intensity of the scattered and exciting light.

Let us take further account of the fact that the source of the initial Stokes photons is not at the point x = L, but is distributed in the medium and represents the ordinary thermal Mandel'shtam-Brillouin scattering by thermal phonons with a scattering coefficient $= kT\overline{\omega_1^4}\gamma^2\beta_S/32\pi^2c^4$. The thermal phonons are incoherent and attenuate in such a way that the scattering light wave is broadened, even if the initial exciting light is coherent and monochromatic. The spectral distribution of the intensity of the light scattered backwards per unit length in a solid angle θ is determined by the expression (it is assumed that $\omega_1 \approx \omega_0$)

$$\mathcal{J}_1(x, \omega_1) = \theta R f(\omega_1)\mathcal{J}_0(x), \quad (66)$$

where

$$f(\omega_1) = \frac{1}{\pi}\frac{\alpha v}{(\bar{\omega}_1-\omega_1)^2+\alpha^2v^2}. \quad (67)$$

In (66), x pertains to the place where the thermal scattering arises. In the linear region (no saturation) the equation for the intensity of the Stokes SMBS is[20]

$$\frac{\partial\mathcal{J}_1}{\partial x} = -G(\omega_1)\mathcal{J}_1(x)\mathcal{J}_0(0) - \theta R f(\omega_1)\mathcal{J}_0(0). \quad (68)$$

Here again we neglect the optical loss. If there is no external source of Stokes radiation, then the boundary condition is of the form $\mathcal{J}_1(x = L, \omega_1) = 0$. From (68) we easily obtain

$$\mathcal{J}_1(0, \omega_1) = \frac{\theta R f(\omega_1)}{G(\omega_1)}\{\exp[\mathcal{J}_0(0)G(\omega_1)L] - 1\}. \quad (69)$$

From (69) in the absence of gain ($\mathcal{J}_0GL \to 0$) we obtain expression (66) for the thermal backwards scattering; when $\mathcal{J}_0(0)G(\omega_1)L \gg 1$, if saturation effects can still be neglected, we obtain

$$\mathcal{J}_1(0, \omega_1) = \mathcal{J}_1^{eq}(L, \omega_1)\exp[G(\omega_1)\mathcal{J}_0(0)L], \quad (70)$$

where

$$\mathcal{J}_1^{eq}(L, \omega_1) = \theta\frac{f(\omega_1)R\mathcal{J}_0(0)}{G(\omega_1)\mathcal{J}_0(0)}. \quad (71)$$

Consequently, the equivalent input signal $\mathcal{J}_1^{eq}$ is the intensity of the backward thermal Stokes scattering per unit frequency over the length of an interaction region equal to the reciprocal of the linear gain, $1/g_{MB} = 1/G\mathcal{J}_0(0)$. From (69) we can determine the widths of the SMBS components. An approximate calculation yields the following result:

$$2\delta\Omega_{MB} = \begin{cases} 2\alpha v & \text{for } G(\bar{\omega}_1)\mathcal{J}_0(0)L \ll 1, \\ 2\alpha v\left[\dfrac{\ln 2}{G(\bar{\omega}_1)\mathcal{J}_0(0)L}\right]^{1/2} & \text{for } G(\bar{\omega}_1)\mathcal{J}_0(0)L \gg 1, \end{cases} \quad (72)$$

where $G(\bar{\omega}_1) = G(\omega_1 = \bar{\omega}_1)$. Let us determine the integral intensity of the Stokes SMBS:

$$\mathcal{J}_1(0) = \int_{-\infty}^{\infty}\mathcal{J}_1^{eq}(L, \omega_1)[\exp(g_{MB}L) - 1]\,d\omega_1. \quad (73)$$

An approximate calculation leads to the following result:

$$\mathcal{J}_1 = \begin{cases} \dfrac{\theta\omega_0^4 kT\gamma^2\beta_S}{32\pi^2c^4}\mathcal{J}_0(0)L & \text{for } g_{MB}L \ll 1, \\ \dfrac{\theta\omega_0^3 kTn^2}{8\pi^3c^2}\dfrac{2\delta\Omega_{MB}}{\Omega_{MB}}\exp[g_{MB}(\bar{\omega}_1)L] & \text{for } g_{MB}L \gg 1. \end{cases} \quad (74)$$

From the second equation of (74) we see that even in the linear region of amplification the integral SMBS intensity increases not exponentially with increasing $g_{MB}L$, but somewhat more slowly, since $\delta\Omega_{MB}$ decreases with increasing $g_{MB}L$. The intensity of the hypersound in SMBS can be calculated by using (65) and (74) (second equation).

We have considered above, in the linear approximation, practically all the characteristics of the SMBS that results from amplification of thermal scattering in media with large acoustic absorption. The solution of the nonlinear problem entails under these conditions appreciable difficulties, because it is necessary to take into account not only the growth of the intensity in space, but also the variation of the spectral width of the scattered light (Tables I and II).

III. RESULTS OF EXPERIMENTAL INVESTIGATION OF STIMULATED MANDEL'SHTAM-BRILLOUIN SCATTERING

1. Preliminary Remarks on the Investigation of Stimulated Mandel'shtam-Brillouin Scattering

In stimulated scattering, just as in thermal scattering of light, one investigates the spectral composition

Table I. Main formulas of the theory of stimulated Mandel'shtam-Brillouin scattering

Main conditions for applicability and observation		Intensity of Stokes SMBS (scattering angle $\vartheta = 180°$)	Intensity of hypersound
Stationary regime $t_0 > J\tau_{ph}$, $L \gg \frac{1}{2\alpha}$, $\lvert E_0\rvert^2 < \lvert E_0\rvert^2_{cr}$	Linear theory $\mathcal{J}_1 \ll \mathcal{J}_0$	$\mathcal{J}_1(0) = \mathcal{J}_1^{eq}\exp[G\mathcal{J}_0(0)\,L]$, $\mathcal{J}_1^{eq} = \theta\,\frac{f(\omega_1)\,R\mathcal{J}_0(0)}{G\mathcal{J}_0(0)}$, $G = \frac{\lvert q\rvert\lvert k_1\rvert\gamma^2\beta_s}{4n^3c}\,\frac{\alpha v^2}{\alpha^2v^2+(\Omega_{MB}-\omega_1)^2}$	$(\mathcal{J}_p)_{max} = \frac{G\mathcal{J}_0(0)}{2\alpha}\,\frac{\Omega_{MB}}{\omega_1}\mathcal{J}_1(0)$
	Nonlinear theory	$\mathcal{J}_0(L) = \mathcal{J}_1(L)+\mathcal{J}_0(L)-\mathcal{J}_1(0)$, $\mathcal{J}_1(L) = \frac{\mathcal{J}_1(0)\left\{1-\frac{\mathcal{J}_1(0)}{\mathcal{J}_0(0)}\right\}}{\exp\left\{\left[1-\frac{\mathcal{J}_1(0)}{\mathcal{J}_0(0)}\right]G\mathcal{J}_0(0)\,L\right\}-\frac{\mathcal{J}_1(0)}{\mathcal{J}_0(0)}}$	
Nonstationary regime	$\mathcal{J}_1 \ll \mathcal{J}_0$, $\lvert E_0\rvert^2 > \lvert E_0\rvert^2_{cr}$, $\frac{\lvert E_0\rvert^2_{cr}}{8\pi} = \frac{2n^2\alpha^2}{\lvert q\rvert\lvert k_1\rvert\gamma^2\beta_s}$, $k_\omega \ll \alpha$	$\mathcal{J}_1 \sim \exp\left[vt(\gamma^{1/2}-\alpha)+\frac{1}{2}\gamma^{1/2}x\right]$, $\gamma = \frac{\lvert q\rvert\lvert k_1\rvert\gamma^2\beta_s}{16\pi n^2}\lvert E_0\rvert^2$	
	$\mathcal{J}_1 \ll \mathcal{J}_0$, $\lvert E_0\rvert^2 \ll \lvert E_0\rvert^2_{cr}$, $t < J\tau_{ph}$, $L > vt$	$\mathcal{J}_1 \sim \exp\left(\frac{\gamma^2\beta_s v\lvert q\rvert\lvert k_1\rvert}{16\pi n^2}\lvert E_0\rvert^2 xt\right)^{1/2}$	$\mathcal{J}_p = \frac{\Omega_{MB}}{\omega_1}\frac{vt}{x}\mathcal{J}_1$
SMBS in an external resonator $\lvert E_0\rvert^2 > \lvert E_0\rvert^2_{thr}$, $\frac{\lvert E_0\rvert^2_{thr}}{8\pi} = \frac{8n^2\alpha k_\omega}{\lvert q\rvert\lvert k_1\rvert\beta_s\gamma^2}$	Near the SMBS threshold	$\lvert E_1\rvert^2 \sim \exp(2\beta t)$, $\beta \approx \frac{c}{n}\left(-k_\omega+\frac{\lvert q\rvert\lvert k_1\rvert\beta_s\gamma^2}{64\pi n^2\alpha}\lvert E_0\rvert^2\right)$	$\frac{W_p}{W_1} \approx \frac{\Omega_{MB}}{\omega_1}\frac{k_\omega c}{\alpha n}$
	$\lvert E_0\rvert^2 \gg \lvert E_0\rvert^2_{thr}$	$\lvert E_1\rvert^2 \sim \exp(2\beta t)$, $\beta \approx \frac{\gamma\lvert E_0\rvert}{8n}\left(\frac{\Omega\omega_1\beta_s}{\pi}\right)^{1/2}$	$\frac{W_p}{W_1} \approx \frac{\Omega_{MB}}{\omega_1}$

Notation: $\mathcal{J}_0$ t_0 - intensity and duration of exciting-radiation pulse; $\mathcal{J}_1$, ω_1, $\mathbf{k}_1$ - intensity, frequency, and wave vector of the scattered radiation; L - region of nonlinear interaction; x - coordinate in the $\mathbf{k}_1$ direction; $\mathcal{J}_p$, Ω_{MB}, v, and α - intensity, frequency, velocity, and amplitude absorption coefficient of hypersound, $2k_\omega$ - coefficient of absorption of light; W_1, W_p - energy density of the scattered radiation and of the hypersound; $J = G\mathcal{J}_0(0)L$; $\tau_{ph} = 1/2\alpha v$. The formulas do not take into account the influence of STS on SMBS (see Ch. IV).

Table II. Parameters necessary to calculate the characteristics of the SMBS phenomenon in certain liquids (scattering angle $\vartheta = 180°$), exciting light $\lambda = 6943$ Å).

Substance	ρ, g/cm^3	n	$\gamma = \rho\frac{\partial\varepsilon}{\partial\rho}$	v_0, m/sec	v_f, m/sec*)	f_{MB}, GHz*)	$\tau_\eta' \cdot 10^{10}$, sec*)	$\alpha_f \cdot 10^{-3}$, cm^{-1}*)	$G \cdot 10^8$, cm/w**)
Acetone	0.791	1.356	0.99	1190	1190	4.60	—	4.9	2.2
Benzene	0.879	1.494	1.62	1324	1474	6.34	2.6	6.8	2.8
Water	0.997	1.330	0.82	1486	1486	5.69	—	8,1	0.64
n-Hexane	0.660	1.372	1.07	1083		4.28		6 5	2.2
Methanol	0.791	1,329	0,91	1114	1118	4.26	—	6.5	1.5
Carbon disulfide	1.262	1.616	2.37	1158	1247	5.80	22	1.6	15
Carbon tetrachloride	1.595	1.456	1,35	920	1021	4.28	0.86	18	0.58
Ethyl ether	0.713	1.351	0,99	1000	1000	3.89	—	5.8	2.4

*Data obtained from results or from appropriate extrapolation of results of an investigation of the spectrum of thermal Mandel'shtam-Brillouin scattering [64,65] and ultrasound data.

**Stationary gain $G = 13.64\,(\gamma^2\beta_S/\alpha n) \times 10^5$ cm/W.

and its intensity on polarization. In addition, in stimulated scattering one studies certain features peculiar only to this scattering and not possessed by thermal scattering of light.

In Ch. II we described the stationary (linearized and nonlinear) and nonstationary theories of SMBS. In the study of the SMBS intensity, it was necessary to determine which of these cases comes closest to the experimental results. It is also necessary to bear in mind that in backward scattering of light there can occur a temporal instability (generation), although actually this process can be realized only at very high intensity of the exciting light (see formulas (28) and (33)), which has not been attained in most studies of SMBS intensity.

In the study of SMBS in a resonator, it is possible to determine the SMBS "threshold" quite distinctly. Outside a resonator, the SMBS "threshold" is very difficult to determine in practice, since for the scattering to be registered its intensity must be sufficiently large, and consequently the experiment must be performed at exciting-light intensities much higher than threshold.

The SMBS process is accompanied by the occurrence of very intense hypersound, the upper frequency limit of which lies near $\sim 10^{11}$ Hz for a solid and $\sim 10^9$–10^{10} Hz for liquids and gases. The generation of sound of such high frequency in liquids and gases by other methods is so far impossible, and in quartz and sapphire at helium temperatures it is possible to generate artificially hypersound up to frequency $\sim 10^{11}$ Hz, but of very low intensity[25].

The propagation of intense light through a nonlinear medium causes stimulated scattering and many other phenomena, such as self-focusing and defocusing of light, destruction of solid transparent dielectrics, cavitation in liquids, plasma production, etc. The degree to which stimulated scattering is connected with all the foregoing phenomena is still unclear, but this question is being continuously investigated.

Methods of SMBS investigation are quite varied, and we shall mention here only a few of them.

The light sources used for the study of stimulated scattering are lasers based on ruby crystals or on neodymium glass, with Q switching, or else harmonics of these lasers, with power ~1–500 MW and with pulse duration 10–30 nsec*. To investigate SMBS it is necessary that the spectral width of the laser radiation be sufficiently small. In the experiments it usually does not exceed 0.01–0.02 cm^{-1}.

The spectral instruments frequently employed are Fabry-Perot interferometers, high-resolution diffraction spectrographs, and in special cases, when very high resolution is required, the method of heterodyning or quadratic detection of light is used.

Figure 3 shows a typical scheme for the study of the spectra of stimulated scattering of light.

The focusing of a giant pulse with power ~100–200 MW in the interior of the investigated sample by means of a spherical lens makes it possible to obtain an intensity of $\sim 10^6$ MW/cm^2, corresponding to an electric-field intensity of $\sim 10^7$ V/cm in the light wave.

*Recent experiments were performed with ultrashort pulses, $\sim 10^{-3}$ nsec [26].

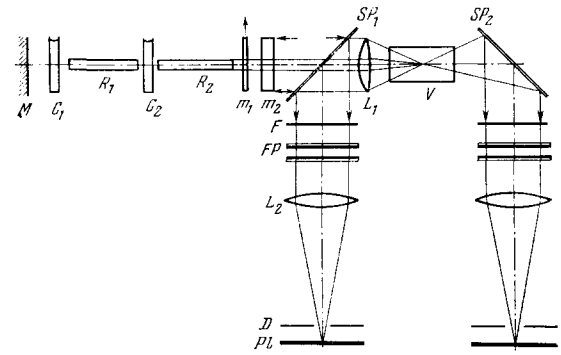

FIG. 3. Optical system for the investigation of the spectrum of stimulated scattering with the aid of a Fabry-Perot interferometer [6]. M – mirror ($R \approx 100\%$); C_1, C_2 – cells with saturable filter; R_1, R_2 – ruby rods; m_1, m_2 – plane-parallel plates (mode selector); Sp_1, Sp_2 – beam-splitting glass plates; L_1 – focusing lens; L_2 – objective; V – investigated sample; FP – Fabry-Perot interferometer; Pl – photographic plate.

When laser radiation is focused with a spherical lens, the maximum scattering intensity can be expected at a scattering angle $\vartheta = 180°$, since the region of nonlinear interaction is maximal for this scattering direction. The use of a cylindrical lens makes it possible to obtain intense SMBS at an angle $\vartheta = 90°$ to the direction of exciting-light propagation*.

The backward-scattered light of the SMBS component enters the still-excited laser, is amplified there, returns to the scattering medium, and may turn out to be intense enough to produce itself an SMBS component. This process can repeat many times. Thus, such a process of successive SMBS leads to the appearance in the spectrum of several components shifted by Ω_{MB}, $2\Omega_{MB}$, etc.

The effect of consecutive SMBS turns out to be parasitic in the study of the intensity of SMBS and in some other cases, and provisions must be made for its elimination†. One of the methods of eliminating the consecutive scattering is to separate the laser and the scattering medium by a distance $l > 2/t_0 c$ (t_0—duration of pulse, c—velocity of light). Another effective method of decoupling the laser and the scattering volume is to employ a polarization shutter‡.

If the scattering medium is located inside an optical resonator[27-30], then the SMBS is produced at a scattering angle ϑ (and $\pi - \vartheta$), equal to the angle between the optical axis of the resonator and the propagation direc-

*In both cases it is difficult to determine the volume of the nonlinear interaction. This is easier to do by using a collimated light beam, compressed in cross section by means of a system of lenses.

†In the case when the scattering is excited by a laser-radiation harmonic, the feedback between the laser and the scattering medium is automatically eliminated.

‡A polarizer (Glan prism) is placed between the laser and the scattering medium, together with a quarter-wavelength plate so oriented that the light focused in the scattering volume is circularly polarized (e.g., right-hand). The light scattered backwards will also be circularly polarized (but to the left). By passing through the same quarter-wavelength plate, the light scattered backwards will be polarized linearly, but with a polarization direction perpendicular to the direction of the polarization of the exciting light, and consequently will not pass through the polarizer into the laser.

tion of the exciting light*.

The diagram of the setup for the observation of SMBS in a resonator is shown in Fig. 4.

Of great significance for the explanation of a number of important questions is measurement of the time variation of the SMBS intensity and a study of the time evolution of the spectrum. For investigations of this type one uses low-inertia photomultipliers, photodiodes, and high-speed oscilloscopes. The time resolution attained in recent investigations of SMBS intensity amounts to 0.3 nsec. To study the kinetics of the SMBS spectrum, one uses electron-optical converters (EOC) operating in the time-sweep mode[31-33]†. Other methodological details of SMBS investigations will be noted during the course of the description of the physical results.

2. Spectral Composition of SMBS

SMBS was discovered in quartz and sapphire crystals by exciting the scattering with a powerful pulse from a ruby laser[5]. This was followed by observation of this phenomenon in liquids[34-36], glasses[37], compressed gases[38-40], and recently in germanium excited with a pulse from a CO_2 laser ($\lambda = 10.6\ \mu$)[100].

The positions of the SMBS components are described by formula (1), and the width of these components should, according to theoretical estimates, be smaller than in thermal scattering‡. The width of the SMBS components, however, was not investigated experimentally as yet.

In the very first experiments on SMBS in liquids and gases, by focusing a laser pulse of power 1—100 MW, the spectrum revealed several Stokes[34-38] and anti-Stokes components. Further investigations of SMBS in quartz crystals, using a focused light pulse of ~500 MW power, up to six Stokes components were observed[41]. In our experiments in liquid carbon disulfide we observed 17 Stokes and two anti-Stokes components[37], and in[44] there were observed 30 Stokes and 15 anti-Stokes components. The appearance of several Stokes SMBS components was interpreted as the result of consecutive scattering, the mechanism of which was described above. The action of the mechanism of consecutive scattering was demonstrated experimentally in experiments in which the SMBS spectrum was time-swept with an electron-optical converter using quartz crystal[32] and gaseous nitrogen[33], and in experiments on the integral intensity of SMBS in liquids[42] and gases[33]. It was shown in these investigations that each succeeding SMBS component is produced with a delay equal to double the time of travel of the light between the scattering medium and the laser.

*In a resonator with axis perpendicular to the propagation direction of the exciting light it is possible to focus light with a cylindrical lens.

† In the study of the kinetics of the SMBS spectrum, the time resolution is limited by the time of establishment of the difraction or interference pattern of the spectral instrument. For a Fabry-Perot interferometer, this time is $\tau_{FP} = N_{eff}h/c \sim 10^{-9}$ sec, where N_{eff} is the number of interfering rays and h is the distance between the interferometer plates.

‡For example, when the intensity of thermal scattering is amplified by a factor e^{20} (J = 20), the width of the SMBS components should be smaller, according to (72), by a factor 5 - 6 than in thermal scattering.

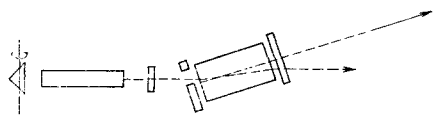

FIG. 4. Experimental setup for the observation of SMBS in an off-axis resonator [27].

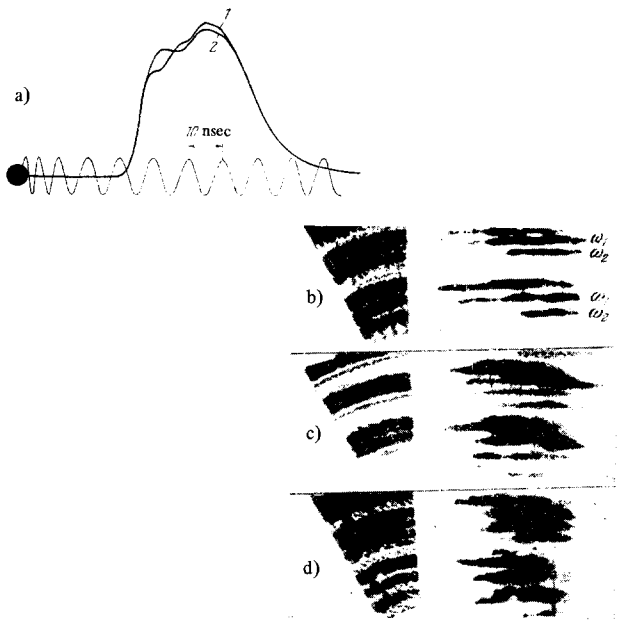

FIG. 5. Interference patterns and oscillograms of SMBS in nitrogen gas (p = 150 atm [33]). Laser power ~50 MW, pulse duration 20 nsec. The laser light is focused with a lens of F= 3 cm. The Fabry-Perot interferometer dispersion region is 0.166 cm^{-1}. In Fig. a oscillogram 1 corresponds to the case of consecutive SMBS (b), oscillogram 2 corresponds to repeated SMBS (c, d) observed at an angle $\vartheta = 180°$. On the left – integral interference patterns, on the right – time-scanned patterns.

Figure 5b shows a time-integrated interference pattern (left) and a time scan (right) of the spectrum of SMBS in nitrogen gas (pressure 150 atm). It is clear from Fig. 5b that the third SMBS component is the result of consecutive scattering.

However, consecutive scattering is not the only cause of appearance of a large number of SMBS components. Indeed, it has been demonstrated that when a light pulse of power ~100 MW is focused in a vessel with liquid acetone, the second Stokes component of SMBS occurs even in the case when the feedback between the scattering volume and the laser is completely eliminated[43]. We assume that in this case the second Stokes component of the SMBS appears in the following manner. The light wave scattered backward and shifted in frequency relative to the laser radiation by Ω_{MB}, without emerging from the region of nonlinear interaction, causes SMBS that is shifted in frequency by $2\Omega_{MB}$ and propagates in the direction of the initial exciting light. Such a scattering will be called repeated. The existence of such a mechanism was demonstrated in a direct experiment of time sweeping with an electron-optical converter, of the SMBS spectrum in nitrogen gas at 150 atm pressure[33]. It is clear from Figs. 5c and d that the first and second

Stokes components of the repeated scattering appear practically simultaneously, unlike the components of the consecutive scattering (Fig. 5b), although the geometry of the setup remained unchanged.

As already stated, it follows from the theoretical analysis that direct generation of anti-Stokes components in SMBS is impossible. It was also noted that the complexity of the SMBS spectrum can lead to ambiguous identification of Stokes and anti-Stokes components[42]. By now, however, sufficient experimental material has been accumulated to be able to state with assurance that the anti-Stokes components are observed[11,33,38,44-46]. Anti-Stokes SMBS components are observed even in those cases when the feedback between the laser and the scattering medium is eliminated[44].

To explain the occurrence of anti-Stokes SMBS components, we can point at least to two causes not accounted for in the theory of Ch. II: a) the presence of repeated SMBS and b) 4-photon interaction in SMBS (optical mixing). Indeed, in repeated scattering, the formation of the second forward-propagating Stokes component is accompanied by the occurrence of an intense backward-propagating hypersonic wave. Scattering of the exciting light by this wave yields a component that is shifted in the anti-Stokes direction and propagates backwards, into the laser. Becoming amplified in the laser, the light of the anti-Stokes component is sufficiently intense to be registered.

Another cause of the appearance of anti-Stokes components may be 4-photon interaction. This phenomenon consists in the fact that in a nonlinear medium two photons of laser radiation are transformed into two scattered photons whose propagation direction and frequency differ from those of the initial photons, but, of course, in such a way as to satisfy the energy and momentum conservation laws. Since the scattered light waves have a much lower intensity than the exciting wave, the different mutual interaction via the refractive index causes the lengths of the wave vectors of the scattered waves to be longer than the wave vector of the exciting light wave* by an amount $\Delta k = \Delta n k/n_0$, where Δn is the nonlinear addition to the refractive index of the medium. The momentum conservation law requires satisfaction of the condition $2\mathbf{k}_0 = \mathbf{k}_1 + \mathbf{k}_2$, where $\mathbf{k}_0$ is the wave vector of the exciting light wave and $\mathbf{k}_1$ and $\mathbf{k}_2$ are the wave vectors of the scattered light waves (Fig. 6). Taking

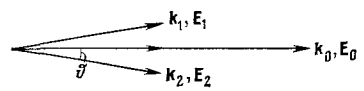

FIG. 6

into account the difference in the lengths of these wave vectors, it is easy to determine the optimal angle of 4-photon interaction:

$$\vartheta_{opt} = \pm \left(\frac{2\Delta k}{k_0}\right)^{1/2} = \pm \left(\frac{2\Delta n}{n_0}\right)^{1/2}. \quad (75)$$

If it is assumed that the entire nonlinear change of the refractive index is due to the orientation of the molecules by the electric field of the light waves, we obtain for the optimal 4-photon interaction angle the expression

$$\vartheta_{opt} = \pm \left(\frac{8\pi N (\alpha_1 - \alpha_2)^2}{45 n^2 kT}\right)^{1/2} |\mathbf{E}_0|,$$

where N is the number of molecules per unit volume and α_1, $\alpha_2 = \alpha_3$ are the principal polarizabilities of the molecule. For $\vartheta = \vartheta_{opt}$, the gain for the Stokes and anti-Stokes components located at a distance $\pm\Omega$ from the exciting line is the same, and equals[47-48]

$$g_{\pm} = -2k_{\omega} + \frac{8\pi |\mathbf{k}_0| N (\alpha_1 - \alpha_2)^2}{45 n^2 kT (1 + \Omega^2 \tau_a^2)^{1/2}} |\mathbf{E}_0|^2; \quad (76)$$

here τ_a is the anisotropy relaxation time. For $E_0 \sim 2 \times 10^7$ V/cm and $\Delta\nu = \Omega/2\pi c = 1$ cm^{-1}, $\tau_a = 2.5 \times 10^{-12}$ sec (τ_a is taken for CS_2[11]) we get $\vartheta_{opt} \sim 2°$ and $g_{\pm} \approx 10^3$ cm^{-1}.

Consequently, in a medium consisting of anisotropic molecules, the weak Stokes and anti-Stokes SMBS waves, which are shifted in frequency by $\pm\Omega_{MB}$ from the exciting line, will become amplified.

The existence of such a mechanism for the appearance of anti-Stokes and for the increase of the number of Stokes components was demonstrated experimentally[45]. In that experiment, the SMBS was excited in fused quartz. The radiation, amplified in a laser and again passing through the quartz sample, consisted of the exciting line and one Stokes component. This radiation was focused into a vessel with carbon bisulfide. The spectrum of the light emerging at an angle $\vartheta \sim 0-10°$ from the cell with the CS_2 contained three anti-Stokes and up to nine Stokes components, corresponding to the SMBS in the fused quartz (Fig. 7, III). The interference pattern of the same spectrum (Fig. 7, IV) shows that each SMBS component corresponding to the fused quartz produces in turn a Stokes and an anti-Stokes component of SMBS in the carbon disulfide. If the carbon disulfide is replaced with water or acetone, other conditions being the same, then the spectrum of the light scattered

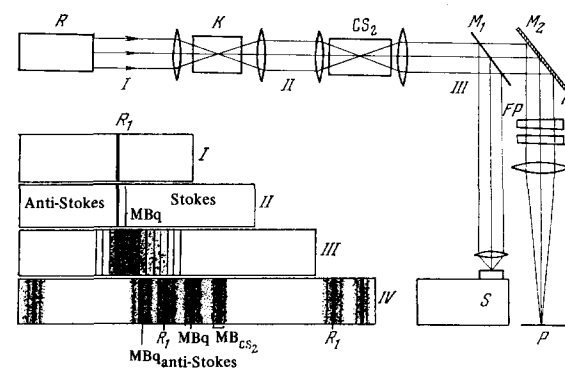

FIG. 7. Spectrogram of SMBS of fused quartz (MBq), passing through water (II) and carbon disulfide (III). Laser light of power ~100 MW is focused with a lens of f = 5 cm into a sample of fused quartz; the light passing through the fused quartz is focused by a system of lenses into a vessel with the liquid. The scattering is observed in the direction of propagation of the exciting light.

*This statement can be readily verified, e.g., for E consisting of a strong wave $\mathbf{E}_0$ and a weak one $\mathbf{E}_1$ (see (11)), and for the expression for the nonlinear polarization

$$\mathcal{P}^{nl} = \frac{\Delta\varepsilon}{4\pi}\mathbf{E} = \frac{\varepsilon_2 \mathbf{E}^2}{4\pi}\mathbf{E} = \frac{\varepsilon_2}{16\pi}[|\mathbf{E}_0|^2(\mathbf{E}_0 e^{i\omega_0 t - i\mathbf{k}_0 r} + 2\mathbf{E}_1 e^{i\omega_1 t - i\mathbf{k}_1 r}) + \mathbf{E}_0^2 \mathbf{E}_1^* e^{i(2\omega_0 - \omega_1)t - i(2\mathbf{k}_0 - \mathbf{k}_1)} + \ldots].$$

It is seen from this expression that the nonlinear addition to the refractive index of the wave $\mathbf{E}_1$ is twice as large as for the wave $\mathbf{E}_0$ ($|\mathbf{E}_0| \gg |\mathbf{E}_1|$).

in the fused quartz does not change after passing through the vessel with the liquid. Replacement of the vessel with the liquid by mirrors with reflection coefficients up to 98% increased the number of Stokes components to three, and no anti-Stokes components appeared at all in this case. A detailed analysis[146] shows that the two mechanisms described above (in some cases it is necessary to consider the possible reflection of light from the surfaces of the optical system), in so far as can be judged at present, play the principal role in the occurrence of the anti-Stokes components.

The process of 4-photon interaction can be realized also as a result of the effective electrostriction in SMBS at small angles. In this case k_1 and k_2 in Fig. 6 are the wave vectors of the Stokes and anti-Stokes Mandel'shtam-Brillouin components, the frequency shift of which is small because the scattering angles are small. The optimal angle of 4-photon interaction due to electrostriction will be determined by the expression

$$\vartheta_{opt} \approx \pm \frac{1}{4} \rho \frac{\partial \varepsilon}{\partial \rho} \left(\frac{2\beta_S}{\pi \varepsilon_0}\right)^{1/2} |E^0|.$$

For example, for a field intensity $E_0 \sim 2 \times 10^7$ V/cm we obtain $\vartheta_{opt} \sim 1°$. Under these conditions, owing to the SMBS, there can occur at small angles a powerful ultrasonic wave of frequency $\sim 10^8$ Hz, the absorption coefficient of which in a solid should be smaller by an approximate factor 10^4 than the absorption coefficient of hypersound of frequency $\sim 10^{10}$ Hz, which is generated in the case of SMBS at 180°. Consequently, the gain of the SMBS should increase by two orders of magnitude compared with the value corresponding to scattering at 180°.

The role of powerful ultrasound and the role of the described mechanism of SMBS at small angles in the process of propagation of a powerful light pulse in a nonlinear medium has not yet been explained.

The Stokes SMBS at small angles in an off-axis resonator (see Fig. 4) was observed in carbon disulfide[27,28]. The resonator axis made a small angle $\vartheta = 0.0433$ rad with the propagation direction of the exciting light. The interference pattern of the scattered light revealed two lines, one of which corresponded to SMBS at an angle $\vartheta = 3.1$ rad ($f_{MB} = 5500$ MHz), and the other, as ascertained by measurements made by the light-heterodyning method, corresponded to scattering at the small angle $\vartheta = 0.0433$ rad ($f_{MB} = 123$ MHz) relative to the propagation direction of the laser radiation. When the intensity of the laser radiation was decreased, it seemed at first that the component corresponding to the large scattering angle disappeared. Estimates by means of formula (18) show that for f = 123 MHz the SMBS threshold should be higher by several times, and consequently the corresponding component should vanish earlier than the component corresponding to f = 5500 MHz*. This conclusion was indeed confirmed experimentally and reported later in[109].

The off-axis resonator made an angle $\vartheta = 0.0691$ rad with the direction of propagation of the exciting light. In CS_2, the SMBS threshold at a small scattering angle ϑ turned out to be higher than the SMBS threshold at an angle $\pi - \vartheta$.

In the investigation of SMBS in such an off-axis resonator, there was observed in the CS_2 a competition between the SMBS process and stimulated Raman scattering[49]. When the laser radiation intensity was gradually increased, an SMBS component first appeared, followed by a line of stimulated Raman scattering, and the SMBS disappeared. This is connected with the fact that when the stimulated Raman scattering appears, the effective optical-loss coefficient for SMBS (see formula (18)) increases and the SMBS threshold increases strongly. With further increase of the intensity of the exciting radiation, when the intensity of the stimulated Raman scattering lines reached saturation, the SMBS components appeared again*.

Investigations of the positions of the SMBS components in liquids[37] and in gases[38,50-52], when the scattering is excited by a focused laser pulse of power ~ 100 MW, revealed that the shift of the SMBS components is smaller than in thermal scattering with low-power light sources, or than in the case of calculation. Although this difference usually does not exceed 10%, such a change in the frequency of the SMBS components is perfectly measurable.

Table III lists the measured values of the shift of the SMBS components in liquid[37] obtained by focusing laser radiation of power ~ 100 MW with a lens (f = 5 cm). Table IV gives the values of these shifts of the components of the consecutive SMBS in compressed gases, with the laser radiation focused by lenses of different focal lengths f, in cases when feedback exists between the laser and the scattering medium and when this feedback is removed[52]. The measurement results show that the mean values of the shifts of the components of the consecutive SMBS in gases are equal to the shifts of the SMBS components in those cases when there is no feedback between the laser and the scattering medium. A dependence of the shift of the SMBS components on the focal length of the lens, and consequently on the intensity of the exciting radiation, was also observed. The physical reason for this dependence is not quite clear. The shift of the SMBS components compared with the shifts determined from thermal scattering (see Table III) or with the calculated ones (see Table IV) is frequently smaller by an amount exceeding the experimental errors. In gases the hypersound velocity calculated from the shift of the SMBS components turns out to be closer, under definite experimental conditions, to the isothermal value rather than to the adiabatic one as expected[38]. We recall that frequencies for which the propagation of sound changes from adiabatic to isothermal should satisfy the condition[1]

$$\Omega > \Omega_{isoth} = \frac{v^2}{\chi}, \qquad (77)$$

where χ is the temperature-conductivity coefficient. Under the conditions of the discussed investigations $\Omega_{MB} < \Omega_{isoth}$ always, and consequently one can expect

*In the calculation of the gain, the relaxation time of the bulk viscosity of CS_2 was assumed to be [1] $\tau = 2.2 \times 10^{-9}$ sec.

*Quantitative investigations of the threshold values of the length of the interaction region and of the threshold values of the power in SMBS in the resonator and outside the resonator yielded many contradictory results, for different liquids [5,29,30].

Table III. Values of the hypersound velocity in certain substances, obtained from stimulated and thermal Mandel'shtam-Brillouin scattering[37].

Substance	v, m/sec (stimulated scattering)	v, m/sec (thermal scattering)	Substance	v, m/sec (stimulated scattering)	v, m/sec (thermal scattering)
Benzene	1434±15	1474	Nitrobenzene	1546±15	1559
Carbon disulfide	1162±15*) 1232±15	1247	Acetic acid	1105±20	1180

*The upper value of the velocity is obtained from photographs of the SMBS spectrum, when about ten components of consecutive scattering are observed, while the lower value is obtained when two components are observed.

Table IV. Shift of SMBS components in nitrogen gas (p = 125 atm) for lenses with different focal lengths[52]

Focal length of lens, cm	Shift of SMBS components, cm^{-1}			Sound velocity v, m/sec (determined from the value $\Delta\nu_{av}$*)	Focal length of lens, cm	Shift of SMBS components, cm^{-1}			Sound velocity v, m/sec (determined from the value $\Delta\nu_{av}$*)
	I	II				I	II		
	Δν	Δν	$\Delta\nu_{av}$			Δν	Δν	$\Delta\nu_{av}$	
30	0.038	0.040 0.038	0.039	393	5	0.032	0.028 0.029 0.034	0.030	300
20	0.039	0.037 0.037 0.036	0.037	372	3	0.031	0.025 0.027 0.033 0.037	0.030	300
10	0.035	0.036 0.031 0.033	0.033	331					

I - The SMBS was investigated under conditions when the feedback between the laser and the scattering volume was suppressed by means of a polarization (λ/4) shutter.

II - Consecutive production of several SMBS components (the shift Δν is shown for each component).

*The calculated speed of sound is v = 386 m/sec.

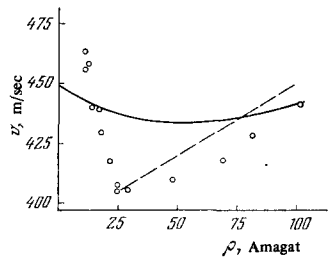

FIG. 8. Dependence of the hypersound velocity in CH_4 (T = 300°K) on the density, obtained from measurements of the position of the SMBS components. Dashed line - result of [50], circles - result of [51], solid line - ultrasound measurements [53].

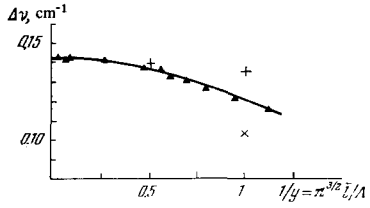

FIG. 9. Dependence of shift Δν of the SMBS component on 1/y (~1/p, p - pressure) in H_2 gas [52]. ▲ - experiment; calculation: + - adiabatic value of hypersound velocity; X - isothermal value of hypersound velocity.

the adiabatic value of the speed of hypersound of frequency Ω_{MB}. Figure 8 shows the dependence of the hypersound velocity, obtained from the shift of the SMBS components in CH_4 (frequency $f_{MB} \sim 10^9$ Hz), on the density[50,51]. In these experiments, laser light with power 20—100 MW was focused by a lens into compressed gas, and there was no feedback between the laser and the scattering volume. It is seen from Fig. 8 (see also[39]) that at high pressures there is satisfactory agreement between the ultrasonic measurements[52] and the data obtained from SMBS. However, when the pressure decreased, a discrepancy appears, reaching a maximum in the region of 25—50 Amagat. With further decrease of the gas pressure, the hypersound velocity again approaches its adiabatic value. A similar dependence is observed also for N_2[51]. All these results have not yet been satisfactorily explained, although different attempts to explain the observed discrepancies were made (see, e.g.,[37,52,54,55]). At sufficiently low hydrogen pressures (below 10 atm), when the pressure decreases, the shift of the SMBS component decreases, as shown in Fig. 9, and this can be attributed to the gradual changeover of the adiabatic sound velocity into isothermal, when the mean free path of the molecules becomes of the order of the length of the sound wave[52].

The assumption that in liquids the effect of the de-

crease of the shift of the SMBS components can be attributed to the effect exerted on the sound velocity by heating of the medium by the laser beam was not confirmed, since a decrease of the shift of the SMBS component was observed also in water[56], although in water, as in gases, the temperature coefficient of the sound velocity is positive. It was shown by the method of light heterodyning[55] that one of the causes of the change of the frequency of the SMBS components may be the existence of feedback between the laser and the scattering medium. In the case of propagation and amplification in a laser of a back-scattered SMBS component, a "pulling" of the component to the neighboring modes of the laser resonator takes place, and the amplification of the SMBS occurs not at the maximum of the Mandel'shtam-Brillouin component, but at a frequency closest to the maximum of the resonator mode. Under different experimental conditions, this effect should give with almost equal probability an increase or a decrease in the shift of the SMBS components, and therefore does not explain the systematically lower values of the shift obtained in the experiment. This effect is even less likely to explain the decrease of the shift of the SMBS component when there is no feedback between the laser and the scattering medium[39,51,52].

It was subsequently demonstrated experimentally[57] that in a single-mode laser and in the absence of feedback between the laser and the scattering medium, the SMBS spectrum in liquids yields for the hypersound velocity values that do not differ from those determined by thermal-scattering measurements. It is proposed[58] that under the same conditions analogous results can be expected also for compressed gases. It should be noted that (although this is not emphasized) in[57] they used of necessity small exciting-light powers. Consequently, in spite of the fact that these results do not explain why the shift of the SMBS components decreases at high powers and in the single-mode regime[52], they do show that the use of a single-mode low-power laser, decoupled from the scattering medium, does make it possible to obtain the correct values of the hypersound velocity from the SMBS spectrum. We propose that one of the reasons of the change in the shift of the Mandel'shtam-Brillouin components in stimulated scattering is the influence of the stimulated temperature scattering (STS) on the SMBS (for details see Ch. IV)*.

If the principal role in the STS process is played by the light-absorption mechanism, than at low SMBS intensities ($\mathcal{J}_{MB} < \mathcal{J}_0/2$), owing to the influence of the STS, the shift of the SMBS component will be larger than in thermal scattering. If on the other hand $\mathcal{J}_{MB} > \mathcal{J}_0/2$, then the shift of the SMBS component will be smaller than in thermal scattering, and it is possible that this is precisely the effect that leads to the observed decrease of the shift of the SMBS components in liquids. In the case when the principal role in the STS component is played by the electrocaloric effect, the situation turns out to be different. When $\mathcal{J}_{MB} > \mathcal{J}_0/2$, the shift of the SMBS components will be larger than in thermal scattering, and the latter case apparently is frequently realized in gases. This explanation is confirmed by certain experimental data (see Ch. IV), but for a final judgement concerning its correctness additional investigations are necessary. Besides this mechanism, the position of the SMBS components may of course be influenced also by other factors.

An experimental investigation of SMBS behind the front of an explosion wave in acetone (pressure ~35 kbar, temperature ~910°K, medium compressed by ~30%), a strong change was observed in the position of the Stokes component of the SMBS compared with its position in uncompressed acetone[101]. In the case of an explosion wave, the shift $\Delta\nu$ (see (1)) consists of shifts due to the following factors: 1) the acoustic velocity and the refractive index behind the wave front, 2) the velocity of the wave front and the difference between the refractive indices ahead and behind the wave front, and 3) the velocity of the medium and the refractive index behind the wave front. The character of the front of the explosion wave affects its intensity distribution in the SMBS component. Undoubtedly, the SMBS can serve as an effective means for the study of the acoustic properties of strongly compressed media in an explosion wave at hypersonic frequencies, and may possibly be useful for the study of the kinetics of the processes occurring in the explosion wave.

SMBS was observed in triglycine sulfate and Rochelle salt[102]* at a threshold lower by one order of magnitude than in quartz and sapphire. The temperature dependence of the SMBS threshold was investigated in Rochelle salt in the vicinity of the temperature of the second order phase transition (upper Curie point). It was observed that the threshold increases smoothly up to the Curie temperature (24.4°C), where it drops jumpwise and then decreases smoothly towards the zone with increasing spontaneous polarization. The variation of the SMBS threshold duplicates in general outline the variation of acoustic loss in this region[103], in agreement with the conclusions of the Landau theory (see[104]). Investigation of SMBS on approaching the critical point of CO_2 has revealed[105], in qualitative agreement with the theory, that the shift of the SMBS component decreases strongly.

Everything stated above pertains to SMBS on longitudinal hypersonic waves. Only in one experiment were

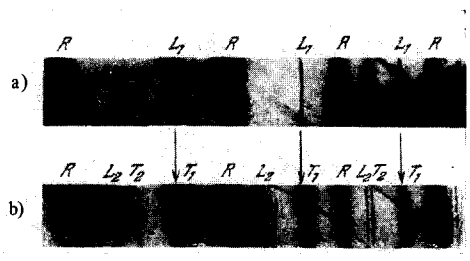

FIG. 10. Interference pattern of SMBS in single-crystal quartz at room temperature (a) and nitrogen temperature (b) [59]. R - exciting line, $L_{1,2}$ - SMBS components at the longitudinal hypersound wave, $T_{1,2}$ - the same at the transverse hypersound wave. Laser power ~250 MW, focusing lens with f = 5 cm.

*It is assumed that the shift of the SMBS component is reckoned from the frequency of the excited radiation.

*No damage occurs in these crystals near the SMBS excitation threshold.

SMBS components observed for transverse (and simultaneously longitudinal) hypersonic waves[59] (Fig. 10). This phenomenon was observed in single-crystal quartz at liquid-nitrogen temperature (−193°C). The crystal was not damaged by focused light of a laser giant pulse with power up to 250 MW. At lower, helium temperatures, no SMBS was produced by transverse hypersound waves. The question of why transverse SMBS components are produced at liquid-nitrogen temperature and not under other conditions still remains unanswered.

3. SMBS Intensity

Great interest attaches to the dependence of the integral light intensity of SMBS on the phonon lifetime (τ_{ph}), the intensity of the exciting light, the length of the region of nonlinear interaction, and the dependence of the instantaneous SMBS intensity on the instantaneous exciting-light intensity. Studies of these questions began only recently. We present below some results of such investigations and compare them with the theory.

a) Dependence of the SMBS intensity on the phonon lifetime. To observe SMBS components under stationary amplification conditions it is necessary to satisfy the condition

$$\frac{1}{\Omega_{MB}} < \tau_{ph} < \frac{t_0}{J}; \qquad (78)$$

here t_0 is the laser pulse duration, $J = g_{MB}L$ is the SMBS light amplification factor. The inequality $1/\Omega_{MB} < \tau_{ph}$ or $\alpha\Lambda < \pi$ is the condition for the existence of discrete components in the thermal and stimulated scattering. The inequality $\tau_{ph} < t_0/J$ follows from (45) (see also (54)) and represents the usual condition of attainment of stationary amplification of SMBS light.

Let us see how the intensity of the SMBS depends on the phonon lifetime. Let the scattered light be amplified in the SMBS process by a factor e^J. Besides the stationary gain, G, we introduce for the nonstationary process an effective gain G*, which can be determined from (46) by means of the expression

$$\frac{1}{2} G^* \mathcal{J}_0 L = \left(\frac{G\mathcal{J}_0 L t}{\tau_{ph}}\right)^{1/2} - \frac{t}{2\tau_{ph}}. \qquad (79)$$

Assuming that in the experiment J has a large and constant* value, we can obtain[60]

$$\frac{G}{G^*} = \frac{[1 + (J/t_0)\,\tau_{ph}]^2}{4\,(J/t_0)\,\tau_{ph}}. \qquad (80)$$

For short laser pulses ($t_0 \ll J\tau_{ph}$), we obtain from (80) $G/G^* = J\tau_{ph}/4t_0$; for long pulses ($t_0 \gg J\tau_{ph}$), the asymptotic value, as follows from the stationary theory, should be $G/G^* \equiv 1$ (Fig. 11). Consequently, if J = const is known, and G/G_{exp} is determined experimentally as a function of the phonon lifetime, then it is possible to obtain the region of transition from the stationary ($G/G_{exp} = G/G^* = 1$) regime to the stationary regime ($G/G_{exp} > 1$). We note that (80) should be valid also for the Stokes stimulated Raman scattering, if τ_{ph} is taken to mean the lifetime of the optical phonon[60].

The intensity of SMBS and of stimulated Raman scattering (RS) in gases (N_2, H_2) was investigated as a function of the phonon lifetime[60]. The lifetime of the optical phonons was changed by four orders of magnitude ($\tau_f \sim 10^{-7}-10^{-11}$ sec) by changing the pressure and temperature of the gas. However, for acoustic phonons, the region of the investigated values of τ_{ph} is much narrower, since at small τ_{ph} it turned out that $\tau_{ph} < 1/\Omega_{MB}$ even before the stationary SMBS regime was attained, and the Mandel'shtam-Brillouin components could not be observed. The general conclusion for the Raman scattering and SMBS is that at J = 30 (this value was determined by the sensitivity of the apparatus) the stationary regime is reached when $\tau_{ph} < 10^{-10}-10^{-9}$ sec (Fig. 11). An estimate of the duration of the nonlinear interaction from the experimentally obtained nonstationary gain following excitation of scattering by a parallel laser beam yields $t_0 = 2 \times 10^{-9}$ sec. The solid curve of Fig. 11 is plotted on the basis of this value of t_0.* Some indication of the cause of such a small t_0, much smaller than the average duration of the laser pulse, can be seen in a remark made in[60], namely that under the conditions of this experiment a temporal change took place in the structure of the laser pulse. Thus, from the results of that investigation it follows that the condition for the transition to the stationary regime, $\tau_{ph} \leq t_0/J$, is actually well satisfied. As expected, at large phonon lifetimes, the effective gain was much smaller than that calculated from the stationary theory. For the same reason, an appreciable decrease is observed in the coefficient of conversion of the exciting-light power into SMBS in carbon bisulfide with picosecond laser pulses[26] compared with the high conversion coefficient obtained with ordinary nanosecond pulses[61].

As follows from (46), in the nonstationary regime, when $t_0 \ll \tau_{ph}$, the SMBS intensity varies like

$$\mathcal{J}_t \sim \exp\left(\frac{\gamma^2 \beta_S v\,|\mathbf{q}|\,|\mathbf{k}_0|}{16\pi n^2}\,|\mathbf{E}_0|^2\, xt\right)^{1/2}$$

and does not depend on the phonon lifetime, in contrast to the stationary regime. Consequently, in the nonstationary case the SMBS threshold is likewise independent of τ_{ph}.

An investigation of the temperature dependence of the SMBS threshold in liquid helium[106] ($\tau_{ph} > 10^{-7}-10^{-9}$ sec) and in crystalline quartz[107] ($\tau_{ph} > 10^{-8}$ sec), and also earlier investigations in certain liquids[30] have shown that such an SMBS regime is actually realized under the conditions indicated above. To register SMBS in liquids, it is necessary to have an amplification by a factor $e^{10}-e^{8}$. Since the phonon lifetime in liquids is $\tau_{ph} \sim 10^{-9}-10^{-10}$ sec, a laser pulse duration $t_0 > 1-10$ nsec is necessary to reach a stationary regime in SMBS.

b) Dependence of the SMBS intensity on the intensity of the exciting light and on the length of the region of nonlinear interaction. Measurements of the dependence of the integral SMBS intensity ($\vartheta = 180°$) on the intensity

*For this purpose, $|E_0|^2$ should change in accordance with the change of the parameters of the scattering medium.

*The experimental data obtained with a focused laser beam lie somewhat higher than the theoretical curve. If account is taken of the influence of diffraction on the calculated value of the nonlinear-interaction volume, then the agreement between the experimental results obtained under different conditions improves.

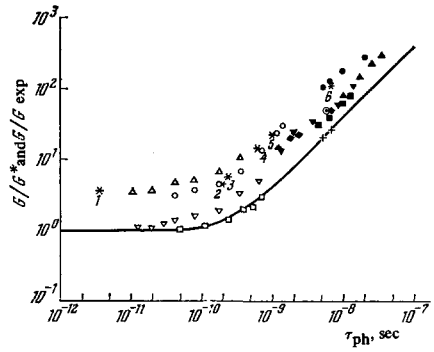

FIG. 11. Dependence of G/G_{exp} and G/G* (solid curve; see (80)) on the phonon lifetime τ_{ph} [60]. 30-cm focus -a) SMBS: ▲,▼- N_2, 300°K; ■, ● - H_2, 77°K; ♦ - CH_4, 300°K; b) RS: Δ, ∇- H_2, 77°K; ○ - H_2, 300°K; c) * - RS: 1 - benzene; SMBS: 2 - CCl_4; 3 - benzene, 4 - water, 5 - acetone, 6 - liquid argon. Parallel beam: + - N_2, SMBS, 300°K; □ - H_2, RS, 300°K.

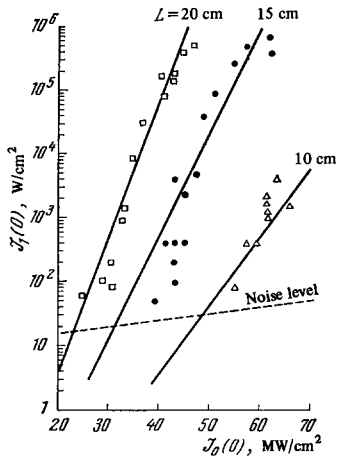

FIG. 12. Dependence of the time-integrated SMBS intensity on the exciting-light intensity in n-hexane [62]. Solid lines - calculation by means of formulas of the stationary theory; experiment: □ - L = 20 cm; ● - L = 15 cm; Δ - L = 10 cm.

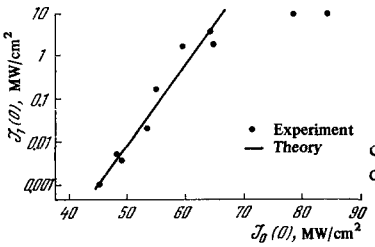

FIG. 13. Measured and calculated SMBS intensity in fused quartz [63].

of the exciting light in liquid n-hexane, methanol, and carbon tetrachloride were made[62] with a giant pulse ($t_0 \sim 15$ nsec) from a single-mode ruby laser. The exciting light was focused with a long-focus lens (f = 1 m) into a vessel with the scattering medium. Between the vessel and the lens, at a distance of 50 cm from the lens, a diaphragm of 1 mm diameter was placed. Such a system made it possible to obtain a sufficiently collimated and homogeneous beam of light. The interference pattern of the scattered light has shown that there was no consecutive SMBS.

Figure 12 shows the dependence of the SMBS intensity $\mathcal{J}_1(0)$ on the intensity $\mathcal{J}_0(0)$ of the exciting light for n-hexane, obtained experimentally for different lengths L of the cell with the liquid, and the results of calculation by means of the formula of the stationary theory (74). Analogous results were obtained[62] for CCl_4 and CH_3OH. Taking into account the difficulty of the experiment, the agreement between the theoretical curves and the experimental points must be recognized to be as perfectly satisfactory.

Measurements were also made of the dependence of the intensity of the Stokes component of SMBS on the intensity of the exciting light in fused quartz[63] (Fig. 13). These measurements together with formulas (60) and (74) have made it possible to obtain the damping coefficient of hypersound ($\alpha = 280\ cm^{-1}$ for $f_{MB} = 2.4 \times 10^{10}$ Hz) in this material. Of course, the use of the linearized theory in[62,63] was possible only because the exciting-light intensities and the lengths L were such that no saturation was reached. It is clear from Fig. 13 that when $\mathcal{J}_0 > 65$ MW/cm² the saturation effect sets in quite clearly and the linearized stationary theory can no longer be used.

In an investigation[66] of the dependence of the SMBS intensity on the length L of the region of nonlinear interaction in n-hexane at sufficiently large L (e.g., at $\mathcal{J}_0 = 7.5$ MW/cm², L > 30 cm), the saturation region was reached*. The saturation of the intensity of the first and second components of consecutive SMBS in fused quartz at high exciting-light intensities was observed also in[67]. In these cases, the SMBS intensity increases much more slowly than predicted by the linearized theory.

c) Dependence of the instantaneous SMBS power on the instantaneous power of exciting light. The intensity of the giant laser pulse, and consequently the SMBS intensity, vary with time, initially increasing from zero to a maximum, and then again decreasing to zero. This temporal variation was used to study the dependence of the instantaneous SMBS power as a function of the instantaneous exciting-light power[68-70]. Following the stationary nonlinear theory, we can write for the SMBS and exciting-life intensities the relations (62), in which we put $G(\omega_1) = G(\bar{\omega}_1) \equiv G$, where

$$G = \frac{\gamma^2 k_0^2 \rho_S}{2n^3 c\alpha} \cdot 10^7 \text{ cm/W}. \qquad (81)$$

In the linear approximation, (62) leads to an exponential growth of $T_1(0)$ as a function of the length and intensity of the exciting light.

In the case of a high conversion coefficient $K = \mathcal{J}_1(0)/\mathcal{J}_0(0) \to 1$ and $G\mathcal{J}_0(0)x \gg 1$, it is easy to obtain $\mathcal{J}(x) = 1/Gx$, and consequently the SMBS intensity does not depend on the exciting-light intensity at large distances from the entrance of the exciting light into the scattering medium. The correctness of this conclusion was confirmed experimentally[68] for CS_2 at $K \approx 0.9$, and a measurement of $\mathcal{J}_1(x)$ was used for an estimate of G.

At high gain, when

$$\exp[(1-K)G\mathcal{J}_0(0)L] \gg K,$$

we get from (62)

$$(1-K)G\mathcal{J}_0(0)L = \ln[(1-K)K] - \ln\left[\frac{\mathcal{J}_1(L)}{\mathcal{J}_0(0)}\right] \equiv C. \qquad (82)$$

*The conclusion that the stationary theory does not hold for n-hexane [66] should apparently be reviewed, since too low a value of α was used in the calculations in [66].

Calculations show that C is approximately constant within a wide range of variation of $\mathcal{J}_0(0)$, L, and G. This statement was verified in[69] in the intervals $\mathcal{J}_0(0) \approx 10-10^3$ MW/cm^2, L = 5—50 cm, and G = $10^{-8}-10^{-7}$ cm/W. Thus, from (82) we get for $\mathcal{J}_1(0)$

$$\mathcal{J}_1(0) = \mathcal{J}_0(0) - \frac{C}{GL}. \quad (83)$$

Of course, it is necessary to satisfy the condition $\mathcal{J}_0(0) > C/GL$. We make the assumption, which usually holds true in reality, that the transverse distribution of the intensity in the exciting light beam is Gaussian, and introduce the power P_0 of the exciting light. Consequently

$$\mathcal{J}_0(0) = \mathcal{J}_0 \exp[-(r/r_0)^2], \quad P_0(0) = \pi r_0^2 \mathcal{J}_0 = S_0 \mathcal{J}_0.$$

Integrating (83) over the cross section of the beam from r = 0 to r_1, determined from the condition $\mathcal{J}_1(0) = 0$ or $\mathcal{J}_0(0) = C/GL$, we obtain for the SMBS power

$$P_1(0) = P_0(0) - \frac{CS_0}{GL}\left[1 + \ln\left(\frac{\mathcal{J}_0 GL}{C}\right)\right]. \quad (84)$$

Owing to the weak (logarithmic) dependence of the second term in (84) on the exciting-light intensity, we conclude that the instantaneous SMBS power in the case of backwards scattering is proportional at the entrance window to the instantaneous input power of the exciting light, and is smaller than this value by a constant quantity (for a given substance, L = const, and $\mathcal{J}_0 GL \gg C$). Further, integrating the first equation of (62) over the beam cross section, neglecting the initial SMBS power $P_1(L)$, and using (84), we get

$$P_0(L) = \frac{CS_0}{GL}\left[1 + \ln\left(\frac{\mathcal{J}_0 GL}{C}\right)\right]. \quad (85)$$

Consequently the power of the exciting light passing through the scattering volume is approximately constant for a given substance if L = const and $\mathcal{J}_0 GL \gg C$. These laws were well confirmed by experimental results for liquids[68,69] for exciting light scattered backwards and passing through the scattering volume.

Figure 14 shows oscillograms (time scans) of an exciting-light pulse (a), of the light scattered backwards in ethyl ether (b), and of the light passing through the scattering medium (c). The SMBS radiation (b) begins from a start rise after the exciting power has reached a certain value. During the remaining part of the laser pulse, the instantaneous power of the SMBS follows the exciting-light power. The instantaneous power of the transmitted light (c) first increases, as does the power of the exciting light, but as soon as SMBS is produced, the instantaneous power of the transmitted light decreases sharply. Then, during the greater part of the pulse, it remains at a constant low level, as follows from (85).

Figure 15 shows the dependence of the instantaneous SMBS power on the instantaneous exciting-light power for ethyl ether, obtained from the oscillogram of Fig. 14. It is seen from Fig. 15 that, with the exception of the initial stage of the pulse (1—2 nsec), the instantaneous SMBS power is proportional to the instantaneous exciting-light power.

A similar situation was observed in CS_2[68,69] and n-hexane[69], the only difference being that for CS_2 at the start of the pulse there is observed a peak in the scattered-light power as a result of the occurrence of stimulated Raman scattering of light. Consequently, in

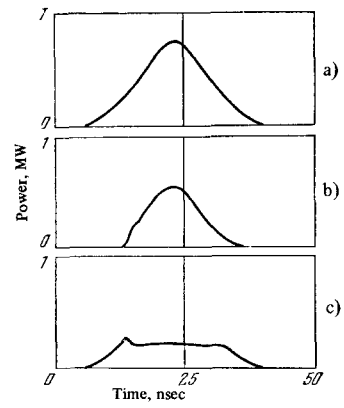

FIG. 14. Power oscillograms of the exciting (a), backward-scattered (b), and transmitted (c) light in ethyl ether [69].

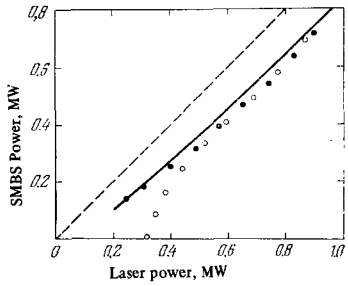

FIG. 15. Instantaneous SMBS power as a function of the increasing (○) and decreasing (●) power of the exciting light in ethyl ether (L = 50 cm) [69].

all these cases, a quasistationary regime is established in the SMBS.

Measurements were also made of the SMBS intensity at small vessel lengths L in CS_2, when no proportionality between $P_1(0)$ and $P_0(0)$ is expected during the duration of the laser pulse. This proportionality can be attained at small values of L by suitable increase of $\mathcal{J}_0(0)$*

The solid curve on Fig. 15 is calculated in accordance with formula (84), and the values of G and C were obtained from experiments in which the dependence of the SMBS power was measured as a function of the distance to the entrance window of the vessel[69]. The obtained values of G (9×10^{-8} cm/W for CS_2, 2×10^{-8} cm/W for ethyl ether, and 1.6×10^{-8} cm/W for n-hexane, accuracy ±50) is in good agreement with those calculated in accordance with the stationary theory. Thus, these experiments show that the stationary theory is applicable to SMBS if the experimental conditions are reasonably chosen, and the SMBS phenomenon can be used to measure G, and consequently to determine the hypersound damping coefficient α.

The most intense conversion of the SMBS exciting-light power occurs, as expected, at the entrance window

*In the experiments of [69] they used collimated light from a ruby laser with maximum intensity $\mathcal{J}_0(0) = 800$ MW/cm^2 for ethyl ether and 500 MW/cm^2 for carbon disulfide. The distance between the vessel with the liquid and the laser was ~4 m, and the components of consecutive SMBS were not produced. An appreciable deviation from proportionality between $P_1(0)$ and $P_0(0)$ in CS_2 occurred at L≤5 cm.

of the vessel[68,69]. In[69], the values obtained for K were 75% in n-hexane (L = 50 cm), 80% in ethyl ether (L = 50 cm), and 90% in CS_2 (L = 30 cm). Even at a distance of several millimeters from the entrance window of the vessel, the SMBS power decreases greatly compared with $P_1(0)$. For example, for CS_2

$$\frac{P_1(x=0.5\,\text{cm})}{P_1(0)}=8\%.$$

Besides the liquids mentioned above, there exist also other in which the instantaneous SMBS power does not follow the instantaneous exciting-light power, but varies jumpwise in time, exceeding at definite instants of time the exciting-light power (e.g., toluene[68]). It is obvious that in this case the stationary stage is not reached.

d) Measurement of the phonon lifetime with the aid of the SMBS phenomenon. Measurement of the gain in SMBS in the stationary regime can be used to determine the hypersound absorption coefficient by means of formula (81), if the other parameters that enter in (81) are known. Apparently, the most suitable procedure for this purpose was proposed and realized in[108]. In this method, two vessels filled with liquid are used (Fig. 16), spaced a small distance apart; they serve as the generator and amplifier of SMBS. The SMBS radiation produced in the generator, which is strongly attenuated by a system comprising a polarizer and a quarter-wavelength plate, is amplified in the amplifier. The exciting radiation P_0, the radiation scattered prior to entry into the amplifier P_i, and the radiation passing through the SMBS amplifier P_a were time-scanned. The small value of the ratio P_i/P_0 ($\sim 10^{-2}$) has made it possible to prevent saturation in the SMBS and to compare the experimental data with the theory of weak SMBS. From this theory, at $t_0 \gg \tau_f$, $t_0 \gg 2L/c$, and $\tau_f \ll L/v$, it follows that

$$\frac{P_a}{P_i}\approx 1+G(\Delta\nu)\mathcal{J}_0 L,$$

where

$$G(\Delta\nu)=\frac{G(0)}{1+(2\Delta\nu/\delta\nu)^2},$$

$\delta\nu$ is the width of the Mandel'shtam-Brillouin component in the thermal scattering, $\Delta\nu$ is the difference of the SMBS frequencies in the generator and amplifier. The hypersound attenuation coefficient can be determined by measuring G(0) ($\Delta\nu = 0$) or by introducing a well determined frequency difference $\Delta\nu$* and finding the $G(\Delta\nu)$ dependence. This makes it possible to determine $\delta\nu$ and to calculate α and τ_{ph} from the width of the $G(\Delta\nu)$ curve. The values of G(0) measured in this manner are in good agreement with the calculated ones. Notice should be taken of the high accuracy of this method of determining α and of the possibility of determining whether the stationary SMBS regime has been reached from the time sweeps of the signals.

4. Generation of Hypersound During the SMBS Process

The frequency of sound generated in SMBS is determined for an isotropic medium by expression (1), or in the general case by the expression

$$\Omega_{MB}=\omega_0\frac{v}{c}\left[(n_1-n_2)^2+n_1n_2\left(2\sin\frac{\vartheta}{2}\right)^2\right]^{1/2}; \quad (86)$$

here ϑ is the scattering angle, n_1 and n_2 are the refractive indices of the exciting and scattered light waves. For anisotropic media, n_1 and n_2 may not be equal to each other. Thus, if we assume for n_1 in the quartz crystal the value of the refractive index for the ordinary beam, and for n_2 that for the extraordinary one, then in scattering in the forward direction ($\vartheta = 0$) we obtain for the frequency of the generated sound $f_{MB} = \Omega_{MB}/2 = 7.5 \times 10^7$ Hz, whereas for scattering at $\vartheta = 180°$ we obtain for f_{MB} the value 2.6×10^{10} Hz. Generation of ultrasound of frequency $f = 7.5 \times 10^7$ Hz in SMBS at an angle $\vartheta = 0$ in X-cut quartz was registered with the aid of a piezoelectric receiver[71].

In SMBS at large angles ($\vartheta \sim \pi$), direct registration of the generated hypersound by ultrasonic methods encounters great difficulties, but such a registration is possible by means of diffraction of the light by the hypersound and was realized in[63].

The upper limit of the hypersound intensity $\mathcal{J}_p$, which can be generated in the SMBS process, is determined by the Manley-Rowe relation $\mathcal{J}_p = (\Omega/\omega_1)\mathcal{J}_1$, where ω_1 and $\mathcal{J}_1$ are the frequency and intensity of the Stokes SMBS. This relation means that the creation of each Stokes photon is accompanied by creation of a phonon. In real experimental conditions, owing to the different limiting factors, the intensity of the hypersound should be smaller than predicted by the Manley-Rowe relation. In the case of short pulses ($vt_0 \ll L$), the Manley-Rowe relation should be decreased by a factor vt_0/L, as follows from the nonstationary theory (formula (53)). Further, because the phonons produced in the SMBS process are strongly absorbed ($\alpha \sim 10^2-10^4$ cm^{-1}), the intensity of the hypersound should also decrease. In the stationary regime, the hypersound intensity is given by relation (65). Consequently, $\mathcal{J}_p$ should be smaller by at least a factor $G_{MB}/2\alpha$ compared with the value given by the Manley-Rowe relation. As already mentioned, the intensity of the hypersound should then reach its maximum value at the entrance (at a distance $x \sim 1/\alpha$) of the exciting radiation into the region of the nonlinear interaction, and should subsequently decrease exponentially in the propagation direction of the exciting light.

An investigation[63] of the intensity of hypersound generated in SMBS ($\vartheta = 180°$) in fused quartz reveals good agreement between experiment and the predictions of the stationary theory. The SMBS was excited by a giant ruby-laser pulse. The intensity of the hypersound was measured with the aid of Bragg diffraction of a beam from a Ne-He laser by a hypersound wave generated in SMBS (the diffraction angle corresponding to the Bragg condition is 126°). On the basis of the first-order approximation, the ratio of the total intensity of the diffracted light $\mathcal{J}_{diffr}$ corresponding to the Bragg condition

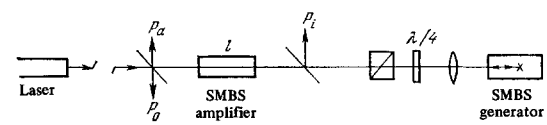

FIG. 16. Diagram of experimental setup for the measurement of the lifetime of phonons with the aid of the SMBS phenomenon [108].

*This can be done, for example, by varying the refractive index and the velocity of the hypersound of the medium of the amplifier or generator of the SMBS.

to the intensity of the incident light J_N is given by the relation

$$\frac{J_{diffr}}{J_N} = \frac{k_N^2 \gamma^2 \beta_S V_3 P_p}{8\pi^2 n^4 v\, dS_N \Delta\vartheta_N}; \quad (87)$$

here k_N, S_N, and $\Delta\vartheta_N$ are the wave vector, cross section, and linear divergence of the Ne-He laser beam; P_p, V_3, and d are the power, volume, and diameter of the acoustic beam. Consequently, by measuring the ratio J_{diffr}/J_N along the nonlinear interaction region it is possible to obtain the dependence of the power in the hypersonic wave P_p on x—the depth of penetration of the light excited by the SMBS.

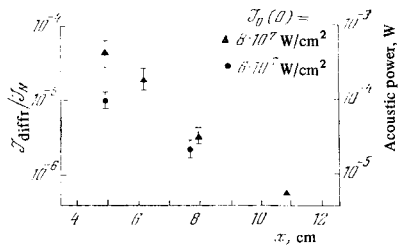

FIG. 17. Spatial profile of the intensity of the hypersonic wave produced in SMBS in fused quartz [63]. The distance is measured from the entrance side of the sample.

Figure 17 shows the spatial distribution of the power of the hypersonic wave in fused quartz at two values of the exciting-light intensity: 80 MW/cm², when the appearance of transients can be expected, and 60 MW/cm², when, as established by an investigation of the SMBS intensity (Ch. III, Sec. 3), a stationary regime is reached. It is seen from Fig. 17 that the power, and consequently also the intensity of the hypersound decreases exponentially with increasing distance from the start of the region of nonlinear interaction. The gain determined from these data turns out to be practically the same as that determined from the SMBS intensity. The maximum acoustic power measured in this experiment is 1.6×10^{-3} W for $J_0 = 60$ MW/cm², which, taking into account the measurement accuracy, is in satisfactory agreement with the value 3.4×10^{-3} W calculated from formulas (65) and (74) of the stationary theory.

Thus, the only measurement made to date of the intensity of the hypersound generated in SMBS in the stationary regime agrees with the measurements of the SMBS intensity and with the theoretical calculation. We note that the value of the power (or intensity) of the hypersound, obtained in this experiment, is much lower (by three orders of magnitude) than the value that follows from the Manley-Rowe relation. At an appreciable excess of the threshold intensity ($g_{MB} \rightarrow \alpha$) and sufficiently long pulses, one can expect J_p to approach to its upper limit $\sim (\Omega_{MB}/\omega_1) J_1$. This regime should set in at high exciting-light intensities and at small hypersound absorption coefficients (e.g., crystals at low temperatures). However, the sound can become nonlinear even earlier, and then the effective absorption coefficient is $\alpha_{eff} = \alpha R$, where α is the usual linear sound absorption coefficient, and R the analog of the Reynolds number, equal to[72]

$$R = \frac{mp}{\eta_{eff}\,\Omega_{MB}} = \frac{mp\Omega_{MB}}{2\alpha v^3 \rho}; \quad (88)$$

here p is the amplitude of the pressure in the sound wave, $\eta_{eff} = 2\alpha v^3 \rho \Omega^{-2}$ is the effective viscosity of the medium at the frequency Ω, and m ~ 1—10 is a parameter characterizing the acoustic nonlinearity of the medium. The acoustic nonlinearity of the medium becomes manifest at $R \gg 1$ or $J_p \gg 2\alpha^2 v^5 \rho / m^2 \Omega_{MB}^2$. From this we find that for a quartz crystal at room temperature ($\alpha = 325$ cm^{-1}) the acoustic nonlinearity begins to come into play at a hypersound intensity $J_p \gg 3 \times 10^2$ W/cm² for a frequency $f_{MB} = 2.6 \times 10^{10}$ Hz. Thus, already at hypersound intensities of several hundred watts, the effective absorption coefficient begins to increase as a result of the development of acoustic nonlinearity. In crystals at low temperatures, the acoustic nonlinearity will develop at still lower hypersound intensities.

When acoustic nonlinearity sets in, there should occur an effective transformation of the hypersound of fundamental frequency into harmonics of higher frequency. The appearance of the second hypersound harmonic $f_{MB} \sim 10^{10}$ Hz of the fundamental frequency $f_{MB} \sim 5 \times 10^9$ Hz was observed in SMBS in water[73]. The SMBS was excited by a focused beam of a ruby laser with power 1—5 MW. Its second harmonic (3470 Å) can be produced by passing a giant ruby-laser pulse through an ADP crystal (conversion efficiency 6%) was incident on a vessel with water collinearly and simultaneously with the ruby-laser emission. Besides the fundamental Stokes SMBS component at $\lambda = 6940$ Å, there was observed the usual thermal scattering at $\vartheta = 180°$ of the light $\lambda = 3470$ Å by the intense second harmonic of the hypersound, for the Bragg condition is satisfied precisely for the second harmonic of the sound, the second harmonic of the light, and the scattering angle $\vartheta = 180°$. The pulses of scattered and exciting light were time-scanned photoelectrically with the aid of high-speed oscilloscopes. The radiation with $\lambda = 6940$ and 3470 Å were separated from each other with the aid of filters.

It can be assumed that further investigation of the hypersound harmonics produced in SMBS will yield interesting results for nonlinear and molecular acoustics.

5. Remarks Concerning Certain Nonlinear Phenomena Accompanying Stimulated Mandel'shtam-Brillouin Scattering

a) Transparent solid dielectrics and crystals. Besides producing SMBS in transparent dielectrics and crystals, intense light also damages these substances[5,11,12,37,59,74-95]. The damage threshold can be higher or lower than the SMBS corresponding to $\vartheta = 180°$ for different media. But the time evolution of the SMBS is apparently faster than that of the mechanical damage, since the latter, in any case, does not screen completely the SMBS light. The damage of transparent dielectrics can be subdivided into 1) damage to the sample surface facing the laser light, 2) damage of the rear surface of the sample, 3) damage in the interior of the dielectric.

The nature of all these various types of damage is still not fully clear, although the literature devoted to this problem is already quite extensive. We are unable to discuss this entire extensive material in detail, and confine ourselves only to an indication of the main trends of the research and some of the conclusions.

Damage of the facing surface is accompanied by a spark on the surface of the sample. This damage has dimensions on the order of several microns, and is frequently surrounded by a dark or brown oreole, having the character of "scald". This phenomenon is apparently connected with the surface dielectric breakdown, which is produced when the dielectric is in vacuum.

A detailed investigation of damage of the rear surface of glasses by a giant laser pulse has led the author of[75] to propose that their cause is the hypersound generated in the SMBS, although there is another opinion concerning this phenomenon. This damage is in the form of small (several tenths of a millimeter) chipping or cleavages. Their threshold is higher than the threshold of damage of the front surface.

The highest threshold is possessed by internal damage (for glasses, higher than 5×10^9 W/cm^2). The following possible damage mechanisms were considered:

1. Damage by hyperacoustic phonons that occur in SMBS[5,75].
2. Absorption of light by superheated liquid glass produced as a result of absorption of hyperacoustic phonons[76].
3. Electrostriction and/or self-focusing[96].
4. Propagation of a light-absorbing shock wave produced in SMBS as the result of the nonlinearity of the sound or other factors[72].
5. Linear absorption of light, particularly by inhomogeneities and inclusions[89].
6. Multiphoton processes of light absorption, ionization, and formation of an electron cascade and plasma[34,82,95].

Each of the foregoing mechanisms, depending on the experimental conditions, can make a contribution to the damage. Thus, in damage of dielectrics with low melting temperature by an ordinary laser pulse of large duration and energy, the main contribution is made apparently by linear absorption of light, i.e., by mechanism 5. However, damage of dielectrics by giant laser pulses, when the pulse energy is low, can usually not be attributed to this mechanism.

In connection with the fact that the damage frequently occurs at lower intensities than the SMBS, it is impossible to explain this phenomenon completely as being due to mechanisms 1, 2, and 4. In various media, damage by means of a giant pulse may be due to different mechanisms or by several of them simultaneously.

The damage most thoroughly investigated was that of silicate glass and quartz by a focused giant laser pulse. The hyperacoustic phonons produced in the SMBS are not the primary cause of damage of these media. An investigation of the time evolution of the damage[88] has shown that it propagates along the light beam with a velocity exceeding $\sim 5 \times 10^7$ cm/sec. It follows from this result that this damage is due to fast processes, such as mechanism 6, for example.

In connection with the fact that part of the damage in glass consists of long filaments ($\sim$1–2 cm)[59,74], it can be assumed that self-trapping of the light beam plays an important role in the damage. One of the causes of damage of silicate glass and quartz is apparently multiphoton absorption (3–4 photons), the formation of an electron cascade and of microplasma with subsequent intense absorption of light[95]. This effect, of course, is facilitated in the case of self-trapping of the light beam.

Investigations of the photoconductivity in glasses and in quartz at a light intensity somewhat lower than needed for damage indicates that multiphoton absorption of light can play a role in the damage of transparent dielectrics[95]. It was observed in our experiments[59], however, that damage of crystalline quartz stops when the temperature is lowered to 80°K or below, although the conditions for multiphoton absorption remain practically the same as at higher temperatures, when damage is observed. It follows from the foregoing that in spite of the large number of investigations, the causes of the damage of transparent dielectrics by a laser beam are still not completely understood.

b) Liquids. In liquids, besides SMBS, there can occur stimulated Raman scattering, stimulated Rayleigh-wing scattering, and stimulated temperature (entropy) scattering of light.

In most cases the threshold for stimulated Rayleigh-wing scattering and stimulated temperature scattering of light are higher than the SMBS threshold.

All the stimulated scattering phenomena are strongly influenced by self-focusing of light rays, if it develops. Liquids are subdivided, purely arbitrarily, into self-focusing (SF) and non-self-focusing (NSF)[97].

In SF liquids, consisting of anisotropic molecules, self-focusing causes the RS and the SMBS to occur simultaneously. When the scattering occurs in a resonator, competition is observed between these two processes, as mentioned in Sec. 2 of this chapter*.

In NSF liquids, as a rule, SMBS sets in at lower exciting-light intensity than all other types of scattering. Therefore these liquids are the most convenient for the study of SMBS, for in this case its character is not distorted by other nonlinear phenomena.

In a focused laser beam of sufficiently high intensity, cavitation and dielectric breakdown can occur in liquids. In a nonfocused beam, when the vessel with the liquid is long and saturation of the SMBS intensity is reached, an intense audible sound is produced[66]. This phenomenon can indicate the formation of an intense acoustic shock wave in SMBS with subsequent conversion of its energy into low frequencies.

c) Gases. The focused light of a giant laser pulse produces breakdown in gases, i.e., strong ionization develops there (see, e.g.,[98]). The breakdown occurs when the electric field intensity in the light beam is $\sim 10^6$–10^7 W/cm. The plasma produced in the breakdown absorbs strongly the laser light. In gases, nonetheless, it is possible to observe in this case several components of consecutive SMBS. This means that the SMBS phenomenon develops earlier than the strongly absorbing plasma, as was demonstrated experimentally in investigations of the time evolution of the SMBS and of the plasma[33].

In compressed gases, besides SMBS, there can be

*There is experimental material pointing to the existence of competition between SMBS and stimulated Rayleigh-wing scattering when the latter phenomenon occurs [43]. The physical nature of the competition between different nonlinear optical phenomena is still not understood.

observed stimulated Raman and stimulated temperature (entropy) scattering.

d) Effect of inverse stimulated Mandel'shtam-Brillouin scattering. If the nonlinear medium is exposed not only to the exciting laser light of frequency ω_0 but also to radiation constituting a continuous spectrum extending to a distance $\Omega_{cont} > \Omega_{MB}$ on the anti-Stokes side, then energy transfer is possible, as the result of the SMBS, from the region of this spectrum $\omega = \omega_0 + \Omega_{MB}$ to the exciting light of frequency ω_0. As a result, a minimum of the intensity will be observed in the continuous spectrum at the frequency $\omega = \omega_0 + \Omega_{MB}$. This effect, called the inverse SMBS, was observed in acetone[99].

IV. STIMULATED TEMPERATURE (ENTROPY) SCATTERING OF LIGHT

The phenomenon of stimulated temperature (entropy) scattering of light (STS)* was first observed in pure liquids in[17]. In this phenomenon, as a result of the interaction between the light wave of the intense exciting light and the weak light waves of the initial thermal scattering by the entropy fluctuations in the nonlinear medium, temperature "waves" are produced and energy is transferred from the exciting radiation to the scattered light wave. Unlike other types of stimulated light scattering, STS can result from two different mechanisms of the nonlinear interaction between the light waves and the medium: 1) the electrocaloric effect and 2) direct absorption of light. Stimulated scattering resulting from the electrocaloric effect will be designated here as STS-I, and stimulated scattering due to absorption of light by STS-II.

The theory of STS-I was developed in[110,111], and the stationary theory of STS-II in[112]. The STS-II phenomenon was observed experimentally in liquids to which absorbing matter was added[113].

1. Theory of STS

In the general case, for both mentioned mechanisms, the action of the electromagnetic waves on the medium in STS is manifest in the occurrence of a heat source. The amount of heat Q released into the medium is proportional to the square of the intensity of the total electric field of the exciting and scattered light waves.

Just as in SMBS, the complete solution of the STS problem can be obtained by simultaneously solving the nonlinear Maxwell's equation and the nonlinear material equation—the temperature-conductivity equation, which is of the form[23]

$$\frac{\partial T_1}{\partial t} - \chi \Delta T_1 = \frac{\dot{Q}}{\rho c_p}. \tag{89}$$

In the case of STS-I (electrocaloric effect[22])

$$\dot{Q} = -\frac{1}{4\pi}\left(\frac{\partial \varepsilon}{\partial T}\right)_p T_0 \mathbf{E}\dot{\mathbf{E}},$$

and in the case of STS-II

$$\dot{Q} = \mathbf{E}\dot{\mathcal{P}} = \frac{1}{2\pi} k_\omega n c \mathbf{E}^2.$$

We introduce the following notation: $2k_\omega = \epsilon''\omega/nc$—the light absorption coefficient, $\mathcal{P}$—the polarization of the medium, T_0—the absolute equilibrium temperature of the medium, T_1—the deviation of the temperature from its equilibrium value, c_p—specific heat of the medium at constant pressure, χ—temperature conductivity of the medium. We shall consider here, however, the more general problem, in order to take into account also the influence of the STS on the SMBS. This can be done by solving the system of equations[111]

$$\left.\begin{aligned} &\frac{\partial^2 u}{\partial t^2} = \nabla^2\left[\frac{1}{\rho\beta_T}(u + \sigma T_1) + \Gamma\frac{\partial u}{\partial t} - \frac{\gamma}{8\pi\rho}\mathbf{E}^2\right], \\ &\frac{\partial T_1}{\partial t} - \chi\nabla^2 T_1 - \frac{\gamma-1}{\sigma}\frac{\partial u}{\partial t} = \frac{1}{4\pi\rho c_V}\left[2k_\omega n c\mathbf{E}^2 - \left(\frac{\partial \varepsilon}{\partial T}\right)_\rho T_0 \mathbf{E}\dot{\mathbf{E}}\right], \\ &\frac{n^2}{c^2}\frac{\partial^2 \mathbf{E}}{\partial t^2} - \nabla^2\mathbf{E} = -\frac{1}{c^2}\frac{\partial^2}{\partial t^2}(Y\mathbf{E}u); \end{aligned}\right\} \tag{90}$$

here $u = \rho_1/\rho$, σ is the coefficient of volume expansion, $\gamma = c_p/c_V = \beta_T/\beta_S$. In the last equation of this system we have neglected the quantity $T_1(\partial\epsilon/\partial T)_\rho$, since $T_1(\partial\epsilon/\partial T)_\rho \ll 1$ Yu. From the system (90) we obtain for STS the same result as obtained by the simultaneous solution of Eq. (89) and the nonlinear Maxwell's equation, but for the SMBS we obtain a result somewhat different from that obtained in Ch. II without taking into account the STS phenomenon.

We solve the stationary problem and consequently we assume that the duration of the exciting-light pulse t_0 exceeds the phonon lifetime τ_{ph} and the time of establishment of the "temperature wave" τ_t, i.e., $t_0 \gg 1/2\alpha v$ and $t_0 \gg 1/\chi q^2$. We assume that the field E consists of a linearly polarized exciting light wave E_0 and a linearly polarized scattered wave E_1.

Frequently in the experiment, the spectral width $\delta\omega_0$ of the exciting light exceeds the width of the line of thermal scattering of the light by the entropy fluctuation and pressure fluctuations, which of course must be taken into account*. This can be done by representing the total field E, the change of temperature T_1, and the relative change of density u in the form

$$\left.\begin{aligned} E &= \frac{1}{2}\int_{-\infty}^{\infty} E_0(\mathbf{r}, \omega_0 - \Omega_1)\exp[i(\omega_0 - \Omega_1)t - i\mathbf{k}_0\mathbf{r}]\,d\Omega_1 \\ &\quad + \frac{1}{2}\int_{-\infty}^{\infty} E_1(\mathbf{r}, \omega_1 - \Omega_2)\exp[i(\omega_1 - \Omega_2)t - i\mathbf{k}_1\mathbf{r}]\,d\Omega_2 + \text{c.c.}, \\ T_1 &= \frac{1}{2}\int_{-\infty}^{\infty} T_1(\mathbf{r}, \Omega - \Omega_3)\exp[i(\Omega - \Omega_3)t - i\mathbf{q}\mathbf{r}] + \text{c.c.}, \\ u &= \frac{1}{2}\int_{-\infty}^{\infty} u(\mathbf{r}, \Omega - \Omega_3)\exp[i(\Omega - \Omega_3)t - i\mathbf{q}\mathbf{r}] + \text{c.c.} \end{aligned}\right\} \tag{91}$$

Substituting (91) in (90) and taking into account the fact that owing to the large gain the spectral width of the scattered light is much smaller than the width of the exciting radiation ($E_1(\omega - \Omega_2) = E_1(\omega_1)\delta(\Omega_2)$, where $\delta(\Omega_2)$ is the δ-function), we get

$$|E_1|^2 = |E_1(\xi = 0)|^2 \exp[g(\Omega)\xi], \tag{92}$$

*STS, and also stimulated concentration scattering in solutions, is sometimes called stimulated scattering at the unshifted frequency, although in either case the maximum of the scattered-light intensity does not coincide with the maximum intensity of the exciting light.

*As a result of the condition $t_0 \gg 1/\chi q^2$, the spectral broadening of the exciting light, due to the finite duration of the pulse, is much smaller than the width of the line of thermal scattering by the entropy fluctuations, but in the case of the total width $\delta\omega_0$ we can have $\delta\omega_0 \gg 1/\chi q^2$.

where ξ is the coordinate in the direction of $\mathbf{k}_1$ and $g(\Omega)$ is the stationary gain, equal to[111]

$$g(\Omega)=\frac{|\mathbf{k}_1|q^2Y}{4\pi n^2\rho}\,\mathrm{Re}\int_{-\infty}^{\infty}\frac{ik_\omega nc+\frac{1}{4}T_0\left(\frac{\partial\varepsilon}{\partial T}\right)_p(\Omega-\Omega_0)}{\rho c_p\beta_S[i(\Omega-\Omega_0)+\chi q^2]}\sigma-\frac{iY}{4}}{(\Omega-\Omega_0)^2-\frac{q^2}{\rho\beta_T}-i(\Omega-\Omega_0)q^2\Gamma-\frac{i(\gamma-1)(\Omega-\Omega_0)q^2}{\rho\beta_T[i(\Omega-\Omega_0)+\chi q^2]}}\times|E_0(\omega_0-\Omega_0)|^2\,d\Omega_0. \quad (93)$$

In (93), $\Omega=\omega_0-\omega_1$ and $\mathbf{q}=\mathbf{k}_0-\mathbf{k}_1$. The obtained general expression for the gain $g(\Omega)$ is valid in the frequency region from $\Omega\sim 0$ to $\Omega\sim\Omega_{MB}$, and consequently takes into account both the SMBS and the STS.

The distribution of the intensity with respect to the frequency of the exciting radiation can be represented with good approximation by the dispersion distribution

$$|E_0(\omega_0-\Omega_0)|^2=\frac{|E_0^m|^2}{\pi}\frac{\delta\omega_0}{\Omega_0^2+\delta\omega_0^2}. \quad (94)$$

Without presenting an analysis of the general cumbersome expression obtained after integrating (93) and taking (94) into account, let us consider two limiting most interesting cases: 1) the scattering spectrum near the frequency of the exciting line, 2) the scattering spectrum near the SMBS frequency.

a) We assume that $q^2/\rho\beta_S=\Omega_{MB}^2\gg\Omega^2$. We can then retain in the denominator (93) only $-q^2/\rho\beta_S$ (when $\Omega>\chi q^2$), and for the gain near the exciting-light frequency we obtain

$$g_t(\Omega)=\frac{|\mathbf{k}_1|\left(\frac{\partial\varepsilon}{\partial T}\right)_p}{8\pi n^2\rho c_p}\left[2k_\omega nc+\frac{1}{2}T_0\chi q^2\left(\frac{\partial\varepsilon}{\partial T}\right)_p\right]\frac{\Omega}{\Omega^2+(\chi q^2+\delta\omega_0)^2}|E_0^m|^2. \quad (95)$$

For the STS, the characteristic quantity is

$$h=\left|\frac{T_0\chi q^2\left(\frac{\partial\varepsilon}{\partial T}\right)_p}{4k_\omega nc}\right|. \quad (96)$$

It is seen from (95) that when $h<1$ and $(\partial\epsilon/\partial T)_p<0$, the anti-Stokes component of the scattering light will become amplified ($g_T>0$ when $\Omega<0$), and when $h>1$ the Stokes component of the scattered light will be amplified ($g_T>0$ when $\Omega>0$). For liquid benzene, for example, the condition $h>1$ means $2k_\omega<5\times10^{-4}\ \mathrm{cm}^{-1}$. The STS gain is maximal at a frequency $\omega_{1\max}=\omega_0\pm(\chi q^2+\delta\omega_0)$. If the spectral width of the exciting radiation $\delta\omega_0$ greatly exceeds the natural line width of the thermal scattering by the entropy fluctuations $\delta\Omega_c=\chi q^2$, i.e., $\delta\omega_0\gg\chi q^2$, then the gain of the STS is smaller by a factor $\chi q^2/\delta\omega_0$ than in the case $\delta\omega_0\ll\chi q^2$.

It follows from (95) that, unlike other types of stimulated scattering, in the case of STS-II ($h<1$) the gain of the anti-Stokes component is the larger the larger the light absorption coefficient, and the gain of the scattered light occurs if the condition $-2k_\omega+g_t\geq 0$ is satisfied, or if

$$\frac{|E_0^m|^2}{8\pi}\geqslant\left|\frac{2\rho c_p(\chi q^2+\delta\omega_0)}{\omega_0\left(\frac{\partial\varepsilon}{\partial T}\right)_p}\right|. \quad (97)$$

The condition (97) was obtained for large values of $2k_\omega$ such that the electrocaloric effect can be neglected.

b) Near the frequency of the SMBS component $\Omega^2\approx\Omega_{MB}^2=q^2/\rho\beta_S\gg(\chi q^2)^2$, neglecting the small terms in (95), we get

$$g_{MB}(\Omega)=\frac{|\mathbf{k}_1|^2}{32\pi n^2}|E_0^m|^2\left\{\Omega_{MB}\beta_S(2-\gamma)\frac{\delta\omega_0+\delta\Omega_{MB}}{(\Omega-\Omega_{MB})^2+(\delta\omega_0+\delta\Omega_{MB})^2}\right.$$

$$\left.+\frac{\sigma}{Y}\frac{\left[4k_\omega nc+T_0\chi q^2\left(\frac{\partial\varepsilon}{\partial T}\right)_p\right](\Omega-\Omega_{MB})}{(\Omega-\Omega_{MB})^2+(\delta\omega_0+\delta\Omega_{MB})^2}\right\}; \quad (98)$$

here $2\delta\Omega_{MB}=\Gamma q^2$ is the half-width of the thermal Mandel'shtam-Brillouin scattering.

The first term of (98), has a maximum at the frequency $\Omega=\Omega_{MB}$, and the second has at $h<1$ a maximum at the frequency $\Omega=\Omega_{MB}+(\delta\omega_0+\delta\Omega_{MB})$ and a minimum at the frequency $\Omega=\Omega_{MB}-(\delta\omega_0+\delta\Omega_{MB})$. Consequently, when $h<1$ there is asymmetry in the gain of the Stokes SMBS relative to the frequency $\Omega=\Omega_{MB}$, the gain being larger on the Stokes side and smaller on the anti-Stokes side relative to the frequency Ω_{MB}.

When $h>1$, the second term has a maximum at a frequency $\Omega=\Omega_{MB}-(\delta\omega_0+\delta\Omega_{MB})$ and a minimum at a frequency $\Omega=\Omega_{MB}+(\delta\omega_0+\delta\Omega_{MB})$, and the total gain will be larger on the anti-Stokes side and smaller on the Stokes side relative to the frequency $\Omega=\Omega_{MB}$. For the case $h<1$, these laws were observed experimentally. We note that such a gain asymmetry can lead to a noticeable shift of the maximum of the SMBS component, so that the measured shift of the Stokes component of SMBS will be larger when $h<1$ and smaller when $h>1$. For an experimental observation of such an effect, the second term in (98) should be comparable in magnitude with the first.

2. Results of Experimental Study of Stimulated Temperature Scattering of Light

As already mentioned above, the STS phenomenon was first observed in liquids to which no special light absorber was added[7]. In that reference, the existence of STS was experimentally demonstrated in the following manner. The spectrum of the stimulated scattering of light was photographed simultaneously at a scattering angle 180° (0°) and at an angle 90°. The liquids used for the investigation were water, methanol, and benzene. In water, there should be no STS, because in the case of water $\gamma=c_p/c_v\approx 1$, $(\partial\epsilon/\partial T)_p$ is small, and the central component in the thermal scattering is practically nonexistent. To the contrary, in benzene the spectral component is very intense, $(\partial\epsilon/\partial T)_p$ is large, and one can expect STS in this liquid. Methanol is intermediate between water and benzene*.

There is no central component on the interference patterns when light is scattered in water at a scattering angle of 90°. In benzene, the central component was observed when the light was scattered at an angle of 90°, and its intensity decreased nonlinearly when the intensity of the exciting light was reduced. The photographs revealed unshifted and shifted fine-structure lines of benzene. Although the observation was carried out at a scattering angle $\vartheta=90°$, the distance between the components corresponded to the scattering angle $\vartheta=180°$. This means that under the conditions of this experiment, the Mandel'shtam-Brillouin components

*A ruby laser of 90 MW power was used. The light was focused into the cell with the investigated liquid by a lens (f = 2.5 cm). Measures were taken to prevent parasitic light from entering the optical setup with the Fabry-Perot interferometer used to register the scattered light at a scattering angle of 90°.

corresponding to $\vartheta = 90°$ were not observed. The appearance of shifted components ($\vartheta = 180°$) can apparently be regarded as scattering of the SMBS components corresponding to $\vartheta = 180°$ by an amplified "temperature wave."

There was the danger that possible inhomogeneities appearing in the liquid at the focus of the laser (e.g., cavitation), might cause a spreading of the exciting light and this can mask the STS. An experiment was therefore performed with methanol, whose hydrodynamic characteristics are such that benzene occupies an intermediate position between it and water. Nonetheless, in methanol, in accordance with the smaller value of $|(\partial\epsilon/\partial T)_p|$ and γ, the intensity of the central component, in the case of scattering at an angle $\vartheta = 90°$ was smaller than in benzene, and vanished when the laser intensity was decreased by a factor of several times. In benzene the central component could still be observed following such a decrease of the intensity.

All the foregoing shows that in these experiments STS was observed in benzene. However, since in these first experiments no detailed investigations were made of the spectral shift of the scattered radiation, it cannot be stated with full assurance whether STS-I or STS-II was observed, although the existence of the STS phenomenon itself was demonstrated*.

a) Observation of STS-I in hydrogen gas. An entirely different method was used to observe STS-I in hydrogen gas in the pressure range 1.5—6.5 atm[52,114]. At these pressures, $\delta\Omega_c > 1/t_0$ and $\delta\Omega_c > \delta\omega_0$, and a maximum could be observed in the STS-I intensity at the half-width of the thermal scattering on the Stokes side relative to the frequency of the exciting light. In this experiment, the gain averaged over the volume was $J = gL \sim 3$, whereas for photographic registration of the effect this quantity should be higher by one order of magnitude. Therefore, to observe the STS we used a trigger mechanism of amplifying the scattered light at the mode of the laser exciting the STS. By a suitable choice of the laser pump power, its operating conditions is made biharmonic by feedback with the scattering volume, and a second laser mode appears at the STS maximum. In the absence of a scattering volume, only one laser emission mode was observed, with width $\sim 10^{-2}$ cm^{-1}.

Figure 18 shows the STS spectra at different hydrogen pressures. At high pressures, the line shape is Lorentzian and its half-width is small. With decreasing pressure, its shape changes, the half-width increases, tending to the Doppler half-width ~ 0.11—0.12 cm^{-1} for hydrogen, as is illustrated in Fig. 19. The dependence of the position of the STS-I maximum on the pressure is in qualitative agreement with the calculations of[115].

In these experiments, in the pressure range from zero to 6.5 atm, an SMBS component was observed frequently in addition to the STS-I line, although special measures were taken to suppress the amplification of the SMBS in the laser with the aid of a suitably chosen mode selector.

b) Study of the STS-II phenomenon. The STS-II phenomenon, connected with the effect of light absorption,

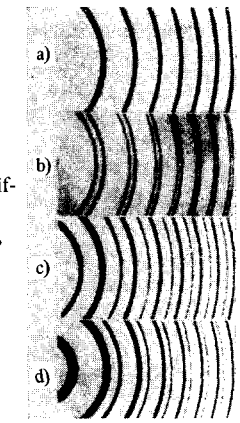

FIG. 18. STS spectrum in hydrogen at different pressures [52,114]. a) R_1 line of ruby laser; b–d) STS spectra at pressures 6.5, 2.5, and 1.5 atm, respectively. The dispersion region of Fabry-Perot interferometer is 0.166 cm^{-1}.

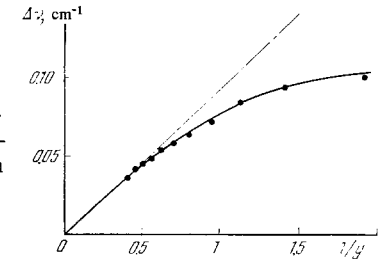

FIG. 19. Shift of STS vs. 1/y (~1/p, p – pressure) in hydrogen [52,114]. Dash-dot line – calculation in accordance with the hydrodynamic theory.

was observed[113,116] in liquid solutions of iodine I_2 in CCl_4 and CS_2, and in the gas mixtures $CO_2 + NO_2$, $N_2 + I_2$, and $N_2 + NO_2$. Addition of I_2 to the liquids and of I_2 and NO_2 to the gases increased the light absorption, leading to an increase of the STS-II gain. The maximum STS intensity was observed at the half-width of the exciting radiation and, as predicted by the theory, on the anti-Stokes side.

STS-II in a liquid solution of I_2 and CCl_4 was investigated also in[117]. The gain was measured as a function of the length of the region of nonlinear interaction L and of the light absorption coefficient $2k_\omega$. The intensity of the scattered light varied like $J_1 \sim \exp(g_t L)$ and remained constant if the quantity $g_t L \sim 2k_\omega L$ remained constant.

The STS-II phenomenon was observed also in liquids* in which laser radiation was focused by a cylindrical lens and the observation was carried out in the direction of the maximum gain at an angle $\vartheta = 90°$ to the direction of laser-radiation propagation[118,119]. The scattered-radiation line is shifted towards the anti-Stokes side relative to the exciting-radiation frequency by approximately 200 MHz, which is in good agreement with the half-width of the exciting radiation $\delta\omega_0 \sim 150$ MHz. It is interesting that when the STS-II line appeared, there was also observed a decrease in the shift of the SMBS component (scattering angle $\vartheta = 90°$) by 200 MHz relative to the laser-radiation frequency. We recall that a decrease of the shift of the SMBS component at a large exciting-radiation intensity was noted long ago and a number of times. This fact can be explained, at any rate for liquids, in the following manner. If the intensity of the laser radiation is so high that the SMBS intensity

*It was assumed initially that STS-I was observed in benzene [17]. This could occur provided $2k_\omega < 5 \times 10^{-4}$ cm^{-1}.

*No absorbing substances were added to the liquids, but they were not specially purified [119].

reaches a value comparable with the intensity of the exciting radiation, and saturation processes come into play in the SMBS, then an intense STS-II is produced both at the frequency of the exciting radiation and at the frequency of the SMBS component. This leads to a shift of both lines towards the anti-Stokes side. Thus, at a high SMBS intensity, owing to the STS effect, the shift of the SMBS component turns out to be smaller by an approximate amount $\delta\omega_0$. The effectiveness of this process is determined by the gain g_t, in which the exciting-radiation intensity should be taken to mean the SMBS intensity. This gain (see (95)) should be larger than that part of the gain of the SMBS (the second term of (98)), which leads to an opposite shift of the frequency of the SMBS component. It follows from (95) and (98) that a decrease of the shift of the SMBS component can be expected if $|E^2_{MB}| > |E_0|^2/2$ or $\mathcal{J}_{MB} > \mathcal{J}_0/2$, where $\mathcal{J}_{MB}$ is the intensity of the Mandel'shtam-Brillouin scattering. If $\mathcal{J}_{MB} < \mathcal{J}_0/2$, then, as follows from (98), the shift of the SMBS component should increase.

c) Study of the influence of STS-II on SMBS at low scattered-light intensities. It follows from the stationary theory (see (98)) that at low scattered-light intensities asymmetry should be observed in the gain of the SMBS component relative to the frequency Ω_{MB}, such that when $h < 1$ the gain is larger on the Stokes side and smaller on the anti-Stokes side relative to the frequency Ω_{MB}. This phenomenon was observed and investigated in a liquid solution of 66% CS_2 + 34% CCl_4, using the setup described in the previous chapter (see Fig. 16)[120]. A vessel 0.20 cm long with a solution of the aforementioned concentration served as an SMBS amplifier. A definite amount of absorbing substance was added to this solution. Therefore $2k_\omega$ changed from the minimum value $2k_\omega \sim 0$ to $2k_\omega = 0.83$ cm^{-1}. The vessel that served as the SMBS generator contained a pure CS_2 + CCl_4 solution, whose concentration was varied, thereby varying the difference between the SMBS generator and amplifier frequencies.

The laser radiation passed through the SMBS amplified and was focused into the SMBS generator. The SMBS light from the generator, attenuated by a system consisting of a polarizer and a quarter-wavelength plate, was returned to the SMBS amplifier and, interacting together with the exciting radiation with the nonlinear medium, became amplified. The gain in the SMBS amplifier, as expected from (98), depends on the difference between the amplifier and generator frequencies. For weak signals ($g_{MB}|E_0|^2 \ll 1$), the ratio of the radiation intensity $\mathcal{J}_a$ prior to entering the SMBS amplifier and the radiation intensity leaving the amplifier $\mathcal{J}_i$ can be written in the form

$$\frac{\mathcal{J}_a}{\mathcal{J}_i e^{-2k_\omega L}} \approx 1 + G(f_{MB} - f)\mathcal{J}_0 L, \qquad (99)$$

where $\mathcal{J}_0$ is the intensity of the exciting radiation, $f = \Omega/2\pi$, G is the gain per unit intensity of the exciting light:

$$G(f_{MB} - f) = \frac{8\pi}{cn^2} \frac{g_{MB}(f_{MB} - f)}{|E_0|^2}. \qquad (100)$$

The frequency difference $(f_{MB} - f)$ in (98), (99), and (100) was determined by the frequency difference of the amplifier and SMBS generator. The signals $\mathcal{J}_0$, $\mathcal{J}_a$, and $\mathcal{J}_i$ were time-scanned, and the gain G was determined with the aid of relation (99) for each value of $(f_{MB} - f)$.

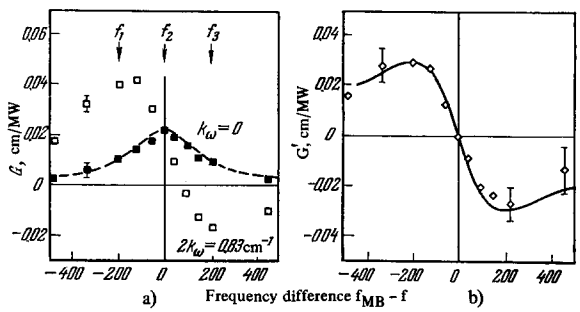

FIG. 20. a) Measured gain of SMBS as a function of the frequency $(f_{MB} - f)$ for a pure liquid ($2k_\omega \sim 0$, dark squares) and for a light-absorbing liquid ($2k_\omega = 0.83$ cm^{-1}, light squares). b) The frequency dependence of the gains shown in Fig. a) for light-absorbing and non-absorbing liquids. Solid curve - theoretical calculations, ◇ - experimental data [120].

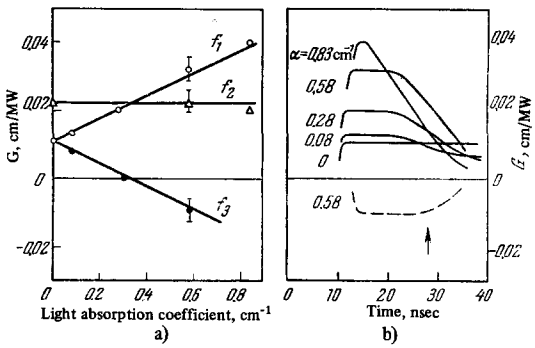

FIG. 21. a) Dependence of SMBS gain on the light-absorption coefficient for three frequencies: ○ - $(f_{mb} - f_1) = -200$ MHz, △ - $(f_{MB} - f_2) = 0$, ○ - $(f_{MB} - f_3) = 200$ MHz. b) Dependence of the gain on the time. Solid curves for $f_{MB} - f_1 = -200$ MHz, dashed curve - $f_{MB} - f_3 = 200$ MHz. The arrow indicates the maximum of the giant laser pulse [120].

Figure 20a shows the stationary gains measured in this manner as functions of the frequency difference $(f_{MB} - f)$ for the pure solution (darks squares) and for the absorbing solution ($2k_\omega = 0.83$ cm^{-1}, light squares), while Fig. 20b shows the dependence of G'—the difference of the gains for the absorbing solution and the pure solution—as a function of the frequency (diamonds), as well as the theoretical $G'(f_{MB} - f)$ curve calculated from the second term of formula (98). The agreement between experiment and theory is undisputed.

Figure 21a shows the dependence of the gain G on the light-absorption coefficient for three frequencies $f_{MB} - f_1 = -200$ MHz, $f_{MB} - f_2 = 0$, and $f_{MB} - f_3 = 200$ MHz. For a correct comparison of the experimental data with the theory, it is necessary to perform the measurements in a stationary regime. To this end, the dependence of the instantaneous intensity $\mathcal{J}_i$ on the instantaneous intensity $\mathcal{J}_0$ was measured, and the dependence of the gain on the time was thus determined (Fig. 21b). The stationary gain was determined from the linear sections of the curves (Fig. 21b) of G against the time*.

*The linear section of the curves of Fig. 21b is followed, at sufficiently long times, by a new time dependence of G. The authors of [120] attribute this to the heating of the scattering medium by the laser radiation.

It follows from all the data presented here that the stationary theory describes the STS phenomenon well if the experimental conditions indeed correspond to the stationarity conditions. The nonstationary processes accompanying STS, however, have hardly been investigated.

In this review we have discussed only the researches known to us dealing with the physical gist of stimulated Mandel'shtam-Brillouin scattering and stimulated temperature scattering or with their study under conditions that are of major physical significance. We did not discuss at all purely technical or practical applications of SMBS. Of course, we could hardly touch upon phenomena accompanying the SMBS and STS, and discussed only some of those which we consider to be the most important.

[1] I. L. Fabelinskii, Molecular Scattering of Light, Plenum Press, N.Y., 1968.

[2] S. A. Akhmanov and R. V. Khokhlov, Problemy nelineinoĭ optiki (Problems of Nonlinear Optics), VINITI, 1964.

[3] N. Bloembergen, Nonlinear Optics, W. A. Benjamin Inc., N.Y., 1965.

[4] E. I. Woodbury and W. K. Ng, Proc. IRE 50, 2367 (1962).

[5] R. Y. Chiao, C. H. Townes and B. P. Stoicheff, Phys. Rev. Lett. 12, 592 (1964).

[6] D. I. Mash, V. V. Morozov, V. S. Starunov, and I. L. Fabelinskii, ZhETF Pis. Red. 2, 41 (1965) [JETP Lett. 2, 25 (1965)].

[7] G. I. Zaĭtsev, Yu. I. Kyzylasov, V. S. Starunov, and I. L. Fabelinskii, ibid. 6, 802 (1967) [6, 255 (1967)].

[8] G. A. Askar'yan, Zh. Eksp. Teor. Fiz. 42, 1567 (1962) [Sov. Phys.-JETP 15, 1088 (1962)]; N. F. Pilipetskiĭ and A. R. Rustamov, ZhETF Pis. Red. 2, 88 (1965) [JETP Lett. 2, 55 (1965)].

[9] R. G. Brewer, Phys. Rev. Lett. 19, 8 (1967); Y. Ueda and K. Shimoda, Japan. J. Appl. Phys. 6, 628 (1967).

[10] N. Bloembergen, Amer. J. Phys. 35, 989 (1967).

[11] V. S. Starunov, Investigation of the Spectrum of Thermal and Stimulated Molecular Scattering of Light, Candidate's Dissertation, FIAN (Physics Institute, Academy of Sciences), 1965; Trudy FIAN 39, 151 (1967).

[12] I. L. Fabelinskii and V. S. Starunov, Appl. Optics 6, 1793 (1967).

[13] Y. R. Shen and N. Bloembergen, Phys. Rev. 137, A1787 (1965).

[14] A. Kastler, Comp. rend. 259, 4233 (1964); 260, 77 (1965).

[15] D. L. Bobroff, J. Appl. Phys. 36, 1760 (1965).

[16] H. A. Haus and P. Penfield, J. Appl. Phys. 36, 3735 (1965).

[17] A. Yariv, IEEE J. Quant. Electr. QE-1, 28 (1965).

[18] C. F. Quate, C. D. Wilkinson and D. K. Winslow, Proc. IEEE 53, 1604 (1965).

[19] N. M. Kroll, J. Appl. Phys. 36, 34 (1965).

[20] C. L. Tang, J. Appl. Phys. 37, 2945 (1966).

[21] K. Grob, Zs. Phys. 201, 59 (1965).

[22] L. D. Landau and E. M. Lifshitz, Elektrodinamika sploshnykh sred, Gostekhizdat, 1957 [Electrodynamics of Continuous Media, Addison-Wesley, 1960].

[23] L. D. Landau and E. M. Lifshitz, Mekhanika sploshnykh sred, Gostekhizdat, 1953 [Fluid Mechanics, Addison-Wesley, 1958].

[24] Chin Dong A, Contribution to the Theory of Stimulated Mandel'shtam-Brillouin Scattering, Diploma Thesis, Scientific director S. A. Akhmanov (Moscow State University, 1964).

[25] J. Ilukor and E. H. Jacobson, Science 153, 1113 (1966).

[26] S. L. Shapiro, J. A. Giordmain and K. W. Wecht, Phys. Rev. Lett. 19, 1093 (1967).

[27] H. Takuma and D. A. Jennings, Appl. Phys. Lett. 5, 239 (1964).

[28] D. A. Jennings and H. Takuma, Appl. Phys. Lett. 5, 241 (1964).

[29] E. B. Aleksandrov, A. M. Bonch-Bruevich, N. N. Kostin, and V. A. Khodovoĭ, Zh. Eksp. Teor. Fiz. 49, 1435 (1965) [Sov. Phys.-JETP 22, 986 (1966)].

[30] A. S. Pine, Phys. Rev. 149, 113 (1966).

[31] E. K. Zavoisky and S. D. Fanchenko, Appl. Opt. 4, 1155 (1965).

[32] C. R. Giuliano, Appl. Phys. Lett. 7, 279 (1965).

[33] V. V. Korobkin, D. I. Mash, V. V. Morozov, I. L. Fabelinskiĭ, and M. Ya. Shchelev, ZhETF Pis. Red. 5, 372 (1967) [JETP Lett. 5, 307 (1967)].

[34] R. G. Brewer and K. E. Riechoff, Phys. Rev. Lett. 13, 334 (1964).

[35] E. Garmire and C. H. Townes, Appl. Phys. Lett. 5, 84 (1964).

[36] R. G. Brewer, Appl. Phys. Lett. 5, 127 (1964).

[37] D. I. Mash, V. V. Morozov, V. S. Starunov, E. V. Tiganov, and I. L. Fabelinskiĭ, ZhETF Pis. Red. 2, 246 (1965) [JETP Lett. 2, 157 (1965)].

[38] D. I. Mash, V. V. Morozov, V. S. Starunov, and I. L. Fabelinskiĭ, ibid. 2, 562 (1965) [2, 349 (1965)].

[39] E. E. Hagenlocker and W. G. Rado, Appl. Phys. Lett. 7, 236 (1965).

[40] D. H. Rank, T. H. Wiggins, R. Y. Wick and D. P. Eastman, JOSA 56, 174 (1965).

[41] P. E. Tannenwald, Physics of Quant. Electronics, Conf. Proc., (Ed. P. L. Kelley, B. Lax and P. E. Tannenwald), 1966.

[42] R. G. Brewer and D. C. Shapero, cm.[41].

[43] G. I. Zaĭtsev, Yu. I. Kyzylasov, V. S. Starunov, and I. L. Fabelinskiĭ, ZhETF Pis. Red. 6, 505 (1967) [JETP Lett. 6, 35 (1967)].

[44] R. V. Wick, D. H. Rank and T. A. Wiggins, Phys. Rev. Lett. 17, 466 (1966).

[45] Yu. I. Kyzylasov and V. S. Starunov, ZhETF Pis. Red. 7, 160 (1968) [JETP Lett. 7, 123 (1968)].

[46] N. Goldblatt and M. Hercher, Phys. Rev. Lett. 20, 310 (1968).

[47] V. S. Starunov, Dokl. Akad. Nauk SSSR 179, 65 (1968) [Sov. Phys.-Dokl. 13, 217 (1968)].

[48] R. Y. Chiao, P. L. Kelley and E. Garmire, Phys. Rev. Lett. 17, 1158 (1966).

[49] T. Ito and H. Takuma, Physics of Quant. Electronics, Conf. Proc. (Ed. P. L. Kelley, B. Lax and P. E. Tannenwald), 1966.

[50] D. H. Rank, R. V. Wick and T. A. Wiggins, JOSA 56, 174 (1966).

[51] T. A. Wiggins, R. V. Wick and D. H. Rank, Appl. Opt. 5, 1069 (1966).

[52] D. I. Mash, V. V. Morozov, V. S. Starunov, and I. L.

Fabelinskiĭ, Zh. Eksp. Teor. Fiz. 55, 2053 (1968) [Sov. Phys.-JETP 28, 1085 (1969)].
[53] J. Naury and A. Lacam, J. Phys. et radium 15, 301 (1954).
[54] A. A. Chaban, ZhETF Pis. Red. 3, 73 (1966) [JETP Lett. 3, 45 (1966)].
[55] R. G. Brewer, Appl. Phys. Lett. 9, 51 (1966).
[56] I. M. Aref'ev, V. S. Starunov, and I. L. Fabelinskiĭ, ZhETF Pis. Red. 6, 677 (1967) [JETP Lett. 6, 163 (1967)].
[57] N. R. Goldblatt and T. A. Litovitz, JASA 41, 1301 (1967).
[58] W. M. Madigosky, A. Monkewicz and T. A. Litovitz, JASA 41, 1308 (1967).
[59] S. V. Krivokhizha, D. I. Mash, V. V. Morozov, V. S. Starunov, and I. L. Fabelinskii, ZhETF Pis. Red. 3, 378 (1966) [JETP Lett. 3, 245 (1966)].
[60] E. E. Hagenlocker, R. W. Minc and W. G. Rado, Phys. Rev. 154, 226 (1967).
[61] M. Maier, W. Rother and W. Kaiser, Phys. Lett. 23, 83 (1966).
[62] J. Walder and C. L. Tang, Phys. Rev. 155, 318 (1967).
[63] J. Walder and C. L. Tang, Phys. Rev. Lett. 19, 623 (1967).
[64] D. I. Mash, V. S. Starunov, E. V. Tiganov, and I. L. Fabelinskiĭ, Zh. Eksp. Teor. Fiz. 49, 1764 (1965) [Sov. Phys.-JETP 22, 1205 (1966)].
[65] R. Y. Chiao and P. A. Fleury, Proc. Conf. on Physics of Quantum Electronics (Ed. by P. L. Kelley, B. Lax and P. E. Tannenwald), 1966.
[66] R. G. Brewer, Phys. Rev. 140, A800 (1965).
[67] S. M. Ryvkin, V. M. Rysakov, I. M. Fishman, B. I. Shklovskiĭ and I. D. Yaroshetskiĭ, Fiz. Tverd. Tela 9, 2735 (1967) [Sov. Phys.-Solid State 9, 2148 (1968)].
[68] M. Maier, W. Rother and W. Kaiser, Appl. Phys. Lett. 10, 80 (1967).
[69] M. Maier, Phys. Rev. 166, 113 (1968).
[70] D. Pohl, M. Maier and W. Kaiser, Phys. Rev. Lett. 20, 366 (1968).
[71] H. Hsu and W. Kavage, Phys. Lett. 15, 207 (1965).
[72] A. L. Polyakova, ZhETF Pis. Red. 4, 132 (1966) and 7, 76 (1968) [JETP Lett. 4, 90 (1966) and 7, 57 (1968)].
[73] R. G. Brewer, Appl. Phys. Lett. 6, 165 (1965).
[74] M. Hercher, JOSA 54, 563 (1964).
[75] C. R. Giuliano, Appl. Phys. Lett. 5, 137 (1964).
[76] D. W. Harper, Brit. J. Appl. Phys. 16, 751 (1965).
[77] P. Whiteman and G. W. Wilson, Nature 208, 66 (1965).
[78] T. Bergqvist, B. Kleman and P. Wahren, Ark. Fys. 34, 81 (1966).
[79] L. M. Belyaev, V. V. Nabatov, Yu. V. Pisarevskiĭ, and Yu. V. Shaldin, Kristallografiya 10, 767 (1965) [Sov. Phys.-Crystallogr. 10, 647 (1966)].
[80] J. David and M. Soulié, Compt. Rend. 261, 3567 (1965).
[81] P. V. Avizonis and T. Farrington, Appl. Phys. Lett. 7, 205 (1965).
[82] T. P. Belikova and E. A. Sviridenkov, ZhETF Pis. Red. 1, No. 6, 37 (1965) [JETP Lett. 1, 171 (1965)].
[83] B. M. Ashkinadze, V. I. Vladimirov, V. A. Likhachev, S. M. Ryvkin, V. M. Salmanov, and I. D. Yaroshetskii, Zh. Eksp. Teor. Fiz. 50, 1187 (1966) [Sov. Phys.-JETP 23, 788 (1966)].
[84] N. V. Volkova, V. A. Likhachev, S. M. Ryvkin, V. P. Salmanov, and I. D. Yaroshetskiĭ, Fiz. Tverd. Tela 8, 2668 (1966) [Sov. Phys.-Solid State 8, 2133 (1967)].
[85] V. A. Likhachev, S. M. Ryvkin, V. M. Salmanov, and I. D. Yaroshetskiĭ, ibid. 8, 3432 (1966) [8, 2754 (1967)].
[86] N. V. Volkova, V. A. Likhachev, V. M. Salmanov, and I. D. Yaroshetskiĭ, ibid. 8, 3595 (1966) [8, 2872 (1967)].
[87] D. Olness, Appl. Phys. Lett. 8, 283 (1966).
[88] J. P. Budin and J. Raffy, Appl. Phys. Lett. 9, 291 (1966).
[89] R. A. Miller and N. F. Borrelli, Appl. Opt. 6, 164 (1966).
[90] A. I. Ritus and A. A. Manenkov, ZhETF Pis. Red. 6, 927 (1967) [JETP Lett. 6, 349 (1967)].
[91] G. M. Zverev and A. D. Martynov, ibid. 6, 931 (1967) [6, 351 (1967)].
[92] A. Wasserman, Appl. Phys. Lett. 10, 132 (1967).
[93] V. I. Vladimirov, V. A. Likhachev, S. M. Ryvkin, V. M. Salmanov, and I. D. Yaroshetskiĭ, Fiz. Tverd. Tela 9, 539 (1967) [Sov. Phys.-Solid State 9, 411 (1967)].
[94] E. J. Greco and J. A. Martinelly, J. Amer. Ceram. Soc. 50, 270 (1967).
[95] B. S. Sharma and K. E. Rieckhoff, Canad. J. Phys. 45, 3781 (1967).
[96] R. Y. Chiao, E. Garmire and C. H. Townes, Phys. Rev. Lett. 13, 479 (1964).
[97] N. Bloembergen, P. Lallémand and A. Pine, IEEE J. Quant. Electr. QE-2, 246 (1966).
[98] Yu. P. Raĭzer, Usp. Fiz. Nauk 87, 29 (1965) [Sov. Phys.-Uspekhi 8, 650 (1966)].
[99] S. Dumartin, B. Oksengorn and B. Yodar, Compt. rend. 262, 1680 (1966).
[100] P. Asam, P. Deuflhard and W. Kaiser, Phys. Lett. 27A, 78 (1968).
[101] R. N. Keeler, G. H. Bloom and A. C. Mitchell, Phys. Rev. Lett. 17, 852 (1966).
[102] F. De Martini, Appl. Phys. Lett. 9, 31 (1966).
[103] I. A. Yakovlev, T. S. Velichkina, and K. N. Baranskiĭ, Zh. Eksp. Teor. Fiz. 32, 48 (1957) [Sov. Phys.-JETP 5, 93 (1957)].
[104] I. A. Yakovlev and T. S. Velichkina, Usp. Fiz. Nauk 63, 411 (1957).
[105] B. S. Guberman and V. V. Morozov, Opt. Spektrosk. 22, 673 (1967).
[106] G. Winterling, G. Walda and W. Heinicke, Phys. Lett. 26A, 301 (1968).
[107] W. Heinicke and G. Winterling, Appl. Phys. Lett. 11, 231 (1967).
[108] D. Pohl, M. Maier and W. Kaiser, Phys. Rev. Lett. 20, 366 (1968).
[109] T. Ito and H. Takuma, J. Phys. Soc. Japan 24, 965 (1968).
[110] V. S. Starunov, Phys. Lett. 26A, 428 (1968).
[111] V. S. Starunov, Zh. Eksp. Teor. Fiz. 57 (1969) [Sov. Phys.-JETP 30 (1970), in press].
[112] R. M. Herman and M. A. Gray, Phys. Rev. Lett. 19, 824 (1967).
[113] D. H. Rank, C. W. Cho, N. D. Foltz and T. A. Wiggins, Phys. Rev. Lett. 19, 828 (1967).
[114] I. L. Fabelinskii, D. I. Mash, V. V. Morosov, V. S. Starunov, Phys. Lett. 27A, 253 (1968).
[115] S. Yip and M. Nelkin, Phys. Rev. 135A, 1241 (1964).

[116] T. A. Wiggins, C. W. Cho, D. R. Dietz and N. D. Foltz, Phys. Rev. Lett. 20, 831 (1968).
[117] F. Gires, Sur quelques effets d'interaction non lineare entre la lumière et la matière, Theses (Orsay, 1968).
[118] J. L. Emmett and A. L. Schawlow, Phys. Rev. 170, 358 (1968).
[119] J. L. Emmett and A. L. Schawlow, Paper at Fourth All-Union Symposium on Nonlinear Optics, Kiev, 1968.
[120] D. Pohl, I. Reinhold and W. Kaiser, Phys. Rev. Lett. 20, 1141 (1968).
[121] Yu. E. D'yakov, ZhETF Pis. Red. 9, 487 (1969) [JETP Lett. 9, 296 (1969)].

Translated by J. G. Adashko